6

DEPOSITIONAL ENVIRONMENTS

CHAPTER 6

DEPOSITIONAL ENVIRONMENT

GENERAL

The previous workers mainly concentrated on archaeology, geomorphology and to some extent on palaeoclimate, but the lack of sedimentological information has been a major lacuna in their work. Detailed sedimentological studies were carried out by the present author for delineating the depositional history of the exposed late Quaternary sediment succession in the Mahi valley. To reconstruct the sedimentation history of the Mahi basin area the best exposed lithosections having lateral as well as the vertical variations in the lithofacies were selected. In the alluvial zone of the lower Mahi basin the exposed sediment succession of around 35 m not only provides information on the various sedimentary processes and related depositional environments but also help in reconstructing the late Quaternary palaeoclimate and in assessing the role of neotectonism.

As facies has been the most powerful tool in understanding the ancient sediments and their related depositional environments (Miall, 1988b), individual facies were identified in the field. Facies codes were given on the basis of their internal and external geometry and sedimentary structures. The facies code classification after Miall (1978) was used with minor modifications. Photomosaics of field photographs were used to know the lateral as well as vertical variations in the alluvial architectural assemblage of the exposed sediment succession.

The sediment bodies show large dimensional bedforms that continue for long distances. Therefore various bedforms were identified and were defined as 'Mesoforms' and 'Macroforms'. The classification of Friend (1983) and Miall (1985) was used. According to these workers "The 'Mesoforms' - includes the large scale flow regime bedforms such as dunes, minor channels that are termed as bars - transverse, longitudinal, linguoid and diagonal generated mainly by dynamic flood events and are typically of 1 m - 10 m in dimension . The 'Macroforms' - includes major or large channels, compound bars; reflects cumulative effects of many dynamic events and are typically of 10 m - 10 km in dimension".

The 2-dimensional outcrops show well developed alluvial architecture assemblage in the lower Mahi basin. The succession comprises sediments deposited under three major environments viz. fluvial, aeolian and marine. These Quaternary sediment successions provide vital information on the allocyclic (extra-basinal) parameters, that controlled the sedimentation pattern in the basin. The allocyclic parameter, includes climatic changes and tectonic adjustments that operated during Quaternary period. The allocyclic parameters must have influenced the autocyclic (intra-basinal) processes, that might have caused the change in channel morphology, variations in sediment discharges, change in sediment size, change in valley slope, change in fluvial regime, change in flow trends, channel avulsion or migration resulting in aggradation (Miall, 1986; Kraus and Middleton, 1987), with intervening periods of non-deposition and sub-aerial weathering.

SEDIMENTARY FACIES

Lithofacies in the lower Mahi valley were recognized and were classified using scheme of Miall (1978a), with minor modifications and additions. Best exposed 2D outcrops were considered for architectural analysis. The succession comprises lithofacies (Table 6.1), viz. Gt, Gp, Sh_1, Sh_2, St, Sim, Sp, Fl and P. Sedimentological studies of individual lithofacies were carried out. Emphasis was mainly given to the granulometry, petrology and clay mineralogy as to understand the mode of deposition, provenance and to some extent the palaeoclimate. Granulometric analysis was carried out for the fine grained unconsolidated lithofacies viz. Sh_1, Sh_2, St and various palaeosol facies. Detailed grain size was done for the type section exposed at Rayka. Systematic sampling was done in the field. The calcified sediments were disaggregated. Of which 50 gm (each) samples were sieved at 0.5∅ interval of ASTM sieve set. Sieve data of these sediments were plotted as cumulative percentages on a log probability paper. Statistical parameters were calculated and analyzed using graphic presentations. Histograms were plotted for various lithofacies, as to understand the dominant grain size and nature of sorting (Folk, 1968; Pettijohn, 1968). Clay mineralogical studies were carried following the methods suggested by Grim (1968) and Carver (1971). The oriented clay aggregated slides were prepared and were examined on a Phillips PW '8210 diffractometer with nickel filter copper radiation (Cukα). Goniometer was run between 2θ angle - $4°$ to $30°$ at a scanning speed of $1°$-$20°$ per minute. The various Å values of individual peaks were then correlated with the standard JCPDS data book on clay mineralogy.

TABLE 6.1 : LITHOFACIES DESCRIPTION (After Miall, 1978)

Facies Code	Description	Interpretation
Gp	Single as well as multi storey, normal graded, 4-5 m thick, planar cross-stratified with dips of 15° to 24°, clast size up to 15 cm in maximum diameter	Aggradation along the avalanching slip-faces of a mid-channel bar during bankfull flows.
Gt	Multi-storey normal graded, 0.5 to 3 m thick, trough cross-stratified with dips of 18°, clast size up to 14 cm in maximum diameter. Calcrete clasts dominant.	Downstream migrating trains of sinuous-crested dunes, longitudinal bars. Channel fill.
St	Trough cross-stratified sands, width up to 8 m and thickness between 0.45 to 1.5 m.	Shallow channels forming through avulsions within the river valley
Sh_1	Horizontally stratified sands, laterally extensive, usually 3 m -4.5 m thick. Extensive vertisol formation.	Overbank deposits formed through episodic infrequent floods.
Sh_2	Horizontally stratified silts, extensively calcretized, channel banks not recognizable.	Shallow-valley river deposits with large width to height ratio, or deposits of sheetflood events
Sim	Massive, unstratified silts, texturally homogenous with calcareous nodules. Geomorphic expression as vertical bluffs.	Aeolian loess-like deposits
Fl	Parallel laminated fine silt-sand	Fluvio-marine mouth bars
Sp	Planar cross-statified sand showing heiringbone structure	Tidal sand bars
P	Pedogenic features	Palaeosols

Detailed description and probable mode of deposition of the various lithofacies is as under:

Planar cross-stratified conglomerate (Gp)

Description: The Gp facies is well exposed at Kadana, Simalya, Poicha, Rayka, Sili and Mohommadpura. The facies in upper as well as in lower reaches occur both as solitary sets and as cosets. The facies in upper reaches rests on the basement rocks. Whereas in lower reaches it overlies the intensely pedogenised fractured mud horizon (vertisol). In upper reaches it is comprised of subrounded to rounded quartzities, with granitic and basaltic clasts (Plate 6.1). The quartzite clasts range in diameter between 6 cm - 14 cm. Clasts are well sorted. The thickness of the lithounits varies between 2 m - 3 m. The foresets are normally graded and dip at an angle of 15°-16° due SW-SSW. The grading is well marked by coarse and fine beds ranging in thickness between 18 cm - 20 cm and 5 cm - 8 cm respectively. The lower bounding surface is non-erosive and the contact is transitional.

In the lower reaches the Gp-facies rests over the vertisol horizon (Plate 6.2). Usually the facies is 4 m - 5 m thick and occurs both as solitary sets and as cosets. At places the thickness varies and pinches down to less than half a meter. The lower bounding surface is usually erosive in nature with local 1 m deep and 1.5 m wide scours, but some sites show planar non-erosive surfaces also. The foresets are normally graded, and the thickness of the beds varies between 2.5 cm to 17 cm. The dips of these foresets ranges between 15° to 24°. Topsets are preserved at some places and drape over the underlying dipping foresets. Clast sizes range in diameter between 1.5 cm - 15 cm, consists mainly of calcrete and basaltic clasts. They are moderately sorted and are sub-rounded to rounded in shape. The matrix is dominated by fine sand and silt (mainly of quartz and basalt) alongwith mica flakes. The parting planes of foresets at places shows drapes of clay laminae occurring parallel to the bedding plane.

Thin section studies of the Gp-facies shows dominant calcrete nodules in their clast composition alongwith quartz, feldspars (plagioclase, orthoclase and microcline), sillimanite, mica and rock fragments of basalts and granites. The intergranular space are filled by sparry and micritic cement and are termed as polymictic conglomerate (Pettijohn, 1968). The large feldspar grains are elongated to sub-rounded embedded in a sparry cementing material with a small amount of quartz in the groundmass. The sub-rounded plagioclases show two types of twinning - multiple and carlsbad twinning. These are unaltered poorly rounded and shows cloudy appearance. The large sub-rounded orthoclase feldspar grains are embedded within the sparry cement and are surrounded by sub-rounded calcrete nodules (Plate 6.3). Occasionally, subangular to a granitic fragments (Plate 6.4) and rounded volcanic lithic fragments are seen embedded within the sparry cement (Plate 6.5).

Interpretation: This facies formed due to downstream accretion of avalanching slip faces on an advancing channel bar. Thickness of upto 3 m suggest bankfull flows of around the same magnitude. High flow velocities are also evidenced in the basal scoured erosional surface into the underlying pedogenised sediments. Such facies have been interpreted as representing migrating straight crested transverse bars (Clemente

Plate 6.1 : Close-up view of cosets in the Gp-lithofacies showing well-rounded quartzitic clasts at Kadana

Plate 6.2 : Gp facies at Rayka.

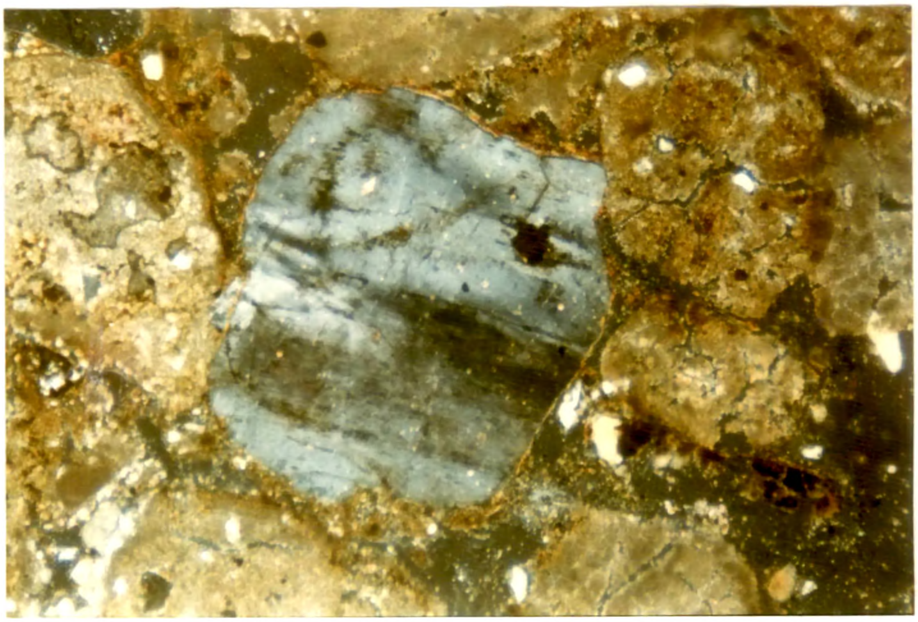

0 0·5 mm.

Plate 6.3 : Photomicrograph of sub-rounded feldspar (orthoclase) and carbonate nodules in a micritic groundmass. (X-Nicols)

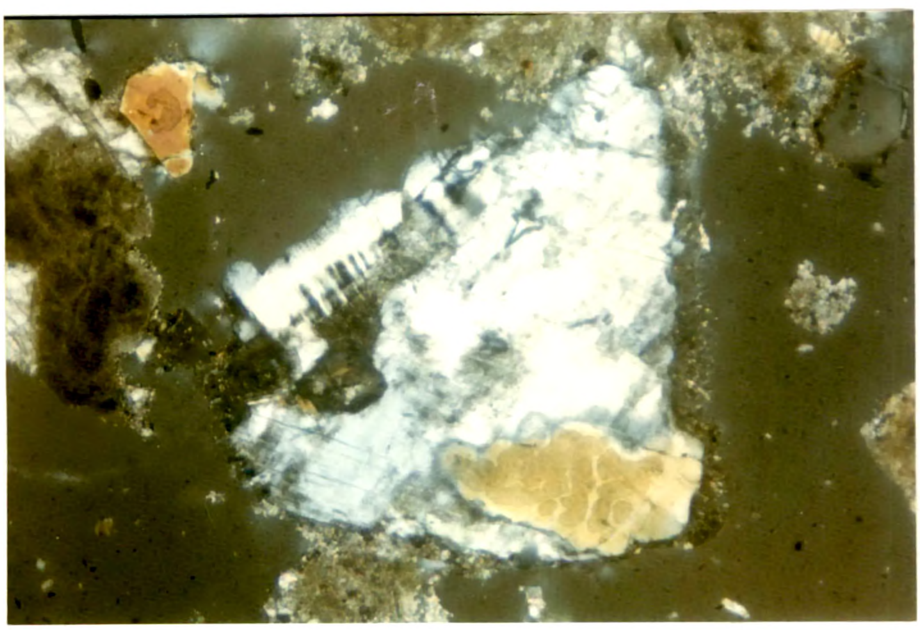

0 0·25 mm.

Plate 6.4 : Photomicrograph of sub-angular granitic grain and sub-rounded carbonate nodules. (X-Nicols)

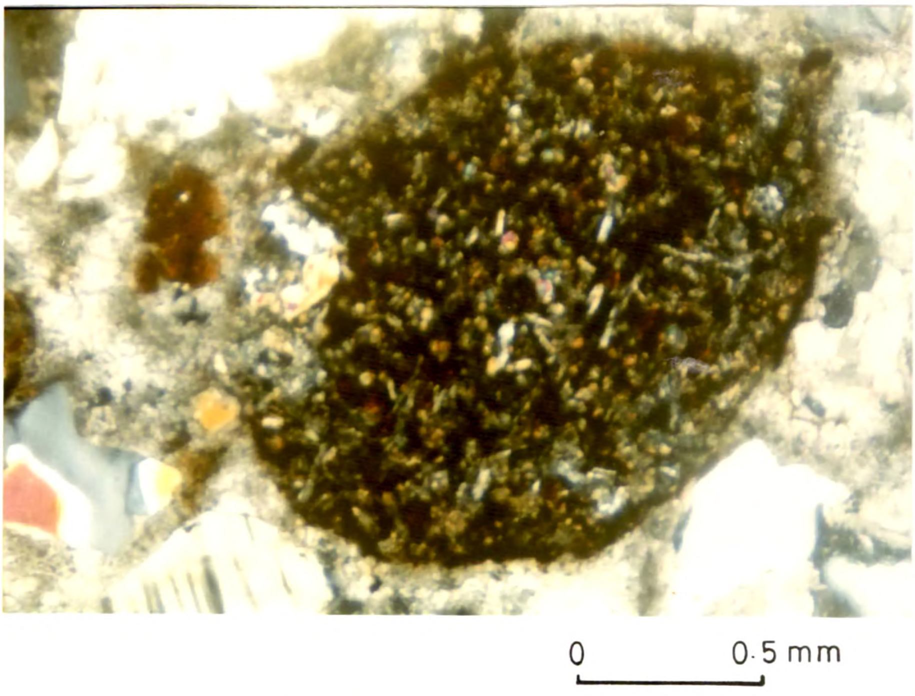

Plate 6.5 : Photomicrograph of sub-rounded basaltic rock fragment and corroded quartz cemented by sparry calcite. (X-Nicols)

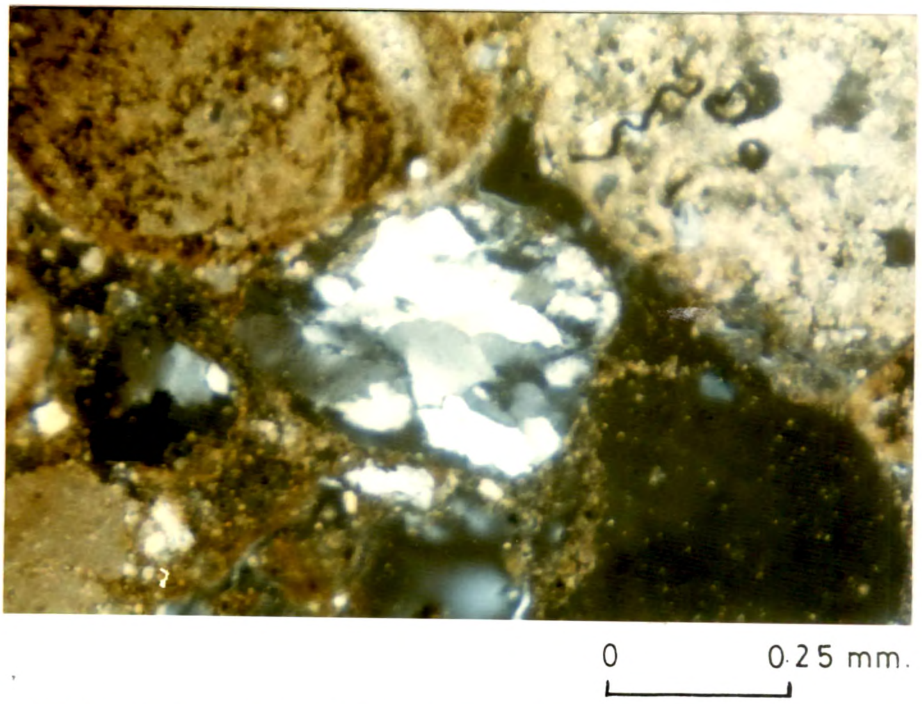

Plate 6.6 : Photmicrograph showing sub-rounded quartzitic grain and carbonate nodules. (X-Nicols)

and Perez-Arlucea, 1993). The geometry of the bedforms suggests that this mesoforms were deposited under waning flood conditions (Miall, 1985). Cementation of this facies may be attributed to local dissolution of the calcrete clast bedload and reprecipitation in the interparticle voids. Where calcrete clasts are less dominate, carbonate charged waters may also have played an important role. Microscopic studies of this facies reveal a short distance transport calcrete or carbonate nodules were derived from the alluvial plain and the other major mineral constituent; quartz and feldspars owe their origin to suggests nearby granitic and basaltic outcrops. The occurrence of angular to sub-angular sillimanite and angular to sub-angular quartz grains suggests nearby contact metamorphic source. The cloudy appearance of the feldspar grains suggests little alteration, whereas the absence of typical carlsbad twinning and rock fragments confirms derivation from the nearby granitic and basaltic source (Young, 1976; Adams *et al.*, 1986).

Horizontally stratified sand (Sh_1)

Description: This facies is well exposed at Poicha, Sili, Bhadarwa, Dodka, Rayka, Phajalpur, Jaspur and Mohommadpura in the lower Mahi valley. Although extensive in development, primary sedimentary structures in the upper portions are obliterated through subsequent pedogenesis. This moderately preserved facies is built up of finely stratified normal graded sand. The sand deposits are bound by laterally continuous horizontal non-erosive surfaces. The facies shows development of orthic carbonate nodules that are found in sub- horizontal parallel bands. Occasionally, the facies shows desiccated cracks which are marked by drab-haloes of greyish green colour. The thickness of the facies varies from 3 m - 4.5 m and is traceable laterally in downstream; farther down they split into thin units of very fine silty sand around 0.5 m thick. The facies at places is cut by sand-troughs of about 2 m - 3.5 m amplitude and 5 m to >15 m in width (Profile 6.1). The fine sand layers and calcrete bands vary in thickness between 30 cm - 35 cm and 15 cm - 20 cm, respectively. Upto fifty bands of calcrete are recorded sandwiched between the underlying Gp facies and overlying Gt facies. The calcrete nodules show differential maturity that is reflected in their carbonate content (whiteness of nodules). The facies is usually capped by soils showing vertic properties. The granulometric analysis and the graphic parameters of these facies show wide variability (Fig. 6.1). The histograms show polymodal nature values ranging between 2.7 Ø - 4.5 Ø, suggests dominance of fine sand and medium to fine silts showing mean average grain size between 2.5 Ø - 4.5 Ø. These contain sand percentage 32%; 55% silts and 13% of clay. The sediments are poor to moderately well sorted.

Interpretation: The facies characteristics suggest an overbank depositional sub-environment. The inherent fineness of the sediment, horizontality and pedogenesis point towards an extra-channel area of aggradation (Bridge, 1984; Clemente and Perez-Arlucea, 1993). The facies was formed through successive episodic flows. Since multiple events of pedogenesis are not observed within the facies it is surmised that such floods were frequent. The presence of St facies within this facies represents the cut and fill channel morphology indicative of channel avulsion in the overbank areas. The alternate fine sand and calcrete bands are suggestive of deposition under highly

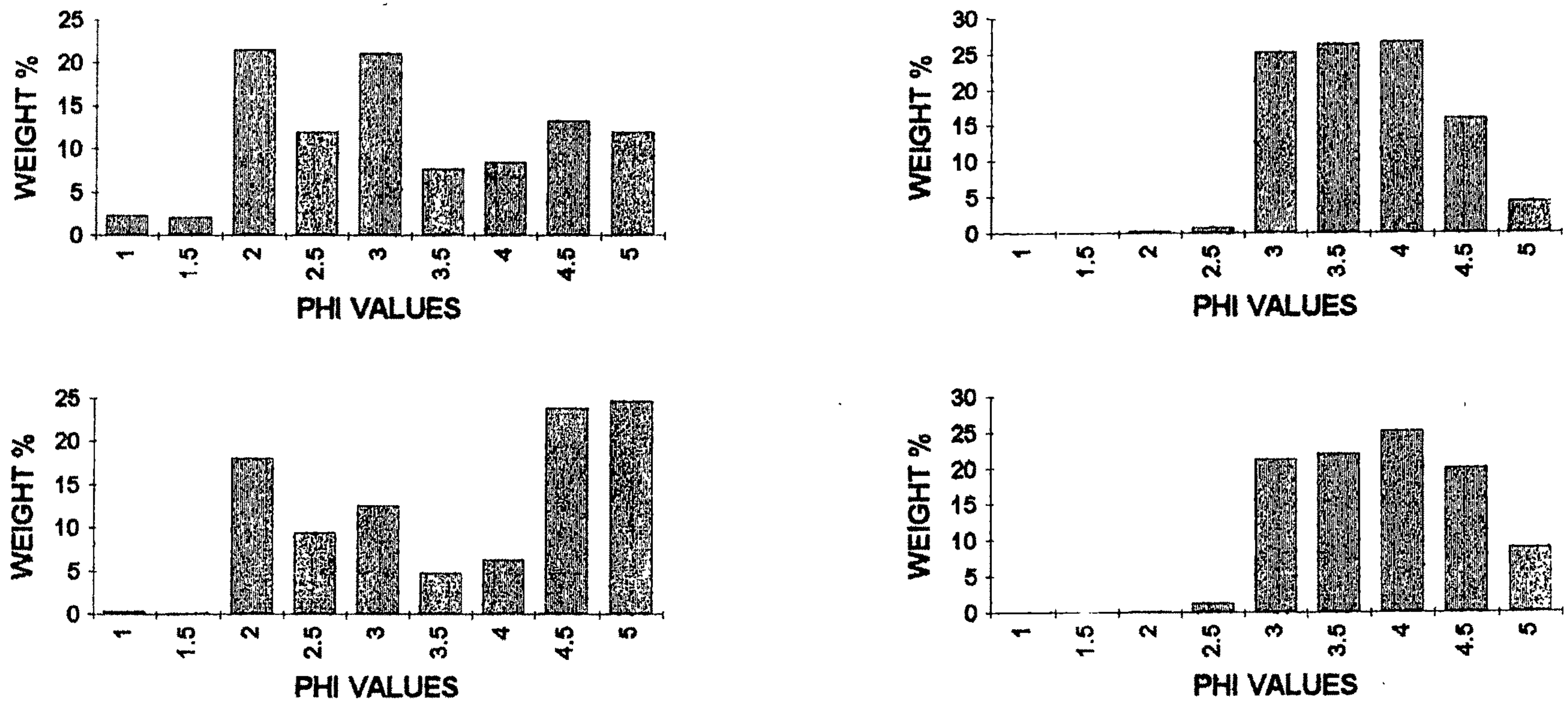

Fig. 6.1 : Representative histograms showing grainsize distribution of the Sh_1 facies

ephemeral channels that transported and deposited sediments as suspension load, followed by calcification during succeeding drier period. The formation of vertic soil also indicates an event of channel avulsion that isolated the area from channel processes and favoured pedogenetic modification of the unit.

Horizontally stratified sand (Sh_2)

Description: This facies is well exposed at Dabka in the lower reaches. Laterally extensive, horizontally stratified sands with calcium rich bands are common in the younger part of the succession (Plate 5.9). The thickness of the unit varies between 4 m to 5 m. This facies occurs as pervasive sheets which extend continuously at Dabka for a distance of 1.5 km. Channel-fills occur within the sheets. Features that might suggest channel bank margins are absent. The granulometric analysis of this facies shows that mean average grain size ranges between 3.33 Ø to 4.5 Ø. The histograms of these sediments show bimodal nature, (values ranging between 3 Ø to 4.5 Ø (Fig. 6.2). Some samples in upper portion of this facies show unimodal nature. The sand, silt and clay percentages are 35%, 55% and 10% respectively. The sediments are moderately to moderately well sorted.

Interpretation: The pervasive nature of the horizontally stratified sands coupled with absence of cross-stratification and channel banks suggests deposition through sheet floods in a ephemeral fluvial regime (Friend, 1983; Eberth and Miall, 1991).

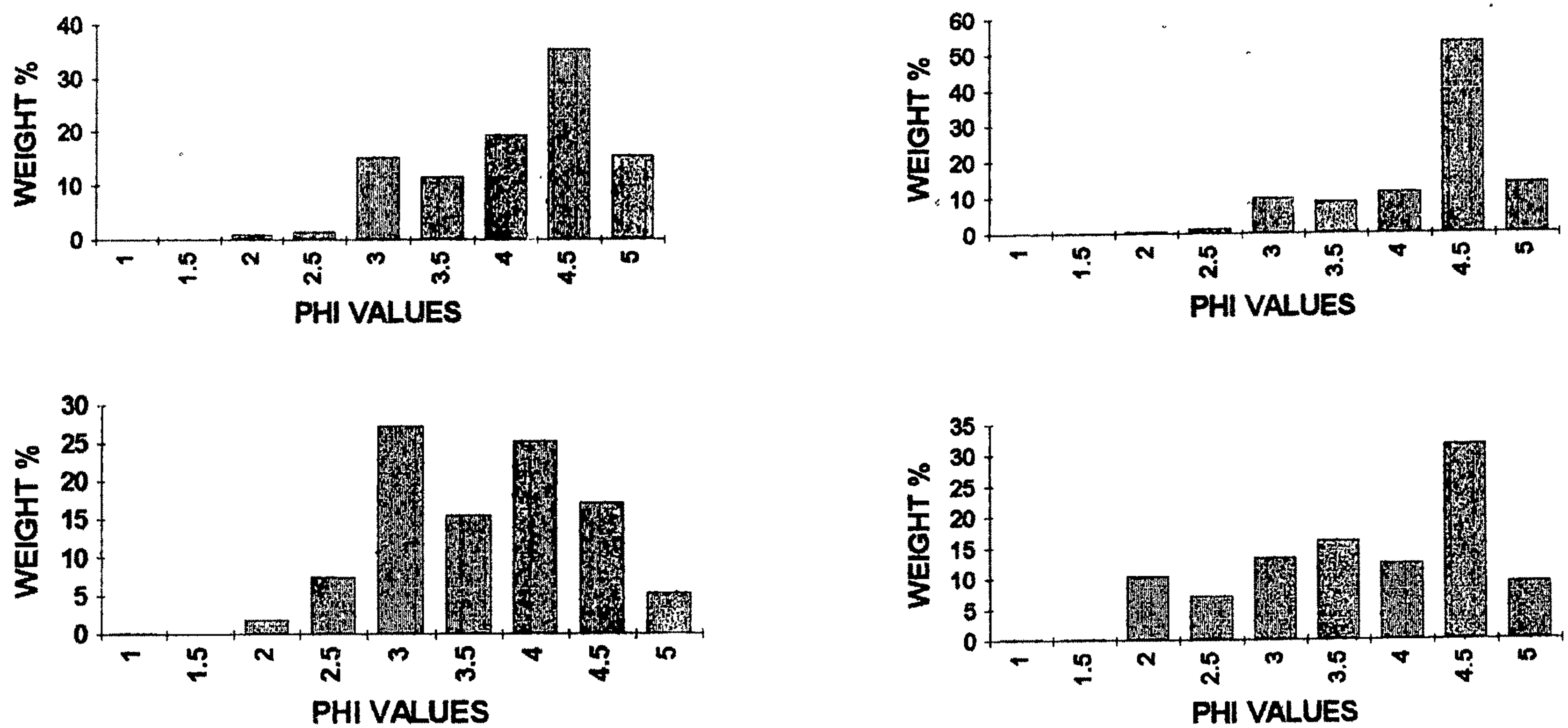

Fig. 6.2 : Representative histograms showing grain size distribution of the Sh_2 facies

Trough cross-stratified sand (St)

Description: The facies is well exposed at Kadana, Poicha, Rayka and Dabka in the Mahi basin. This mesoform comprises sand troughs that vary in amplitude from 0.45 m to 1.5 m and show width of upto 8 m. The facies shows fine internal stratification. The lower bounding surface is erosional. There is a progressive drop in concavity of the bounding surfaces. At one site around Rayka wide shallow troughs (~ 42 m wide) are observed stacked laterally next to each other (Profile 6.1 and 6.6). In this case one of the sides of the predecessor-trough is scoured by the subsequent trough. This facies shows a normal graded sequence. Strata comprise 1.5 cm to 2.5 cm thick sand units and 0.75 cm to 1 cm thick fine silty clay units. Calcium carbonate rich bands are common and occur repetitively through the facies developed along stratification planes. At some intervals 1 cm size clasts of mud are observed. The sediments are dominantly medium to fine sand. The facies is usually (but not always as is observed in the southern section at Dabka) overlain by the Gt calcrete conglomeratic facies, and the transition is gradual. Root casts are present but the density is less. The facies shows average grain size of 3.5 Ø. The sediment package shows 48% of medium to very fine sand, 43% of silts and 9% of clay content in the sand horizons, while finer horizons shows average grain size 4.5 Ø and contain 20% sand, 55% silts and 25% of clay.

Interpretation: This facies is interpreted as deposits of channels (Miall, 1985; 1988a) within the main channel body. The fine laminations within the facies may be due to the sediment being transported in suspension and deposited as a suspension fall-out. Suites of channels positioned next to each other may be interpreted as the result of palaeoflood induced avulsions as has been shown by Malik and Khadkikar (1996). Calcification - (calcretization?) of the facies points to periods of dryness during which groundwater evaporation led to precipitation of calcium carbonate along stratification planes. That these sites were occasionally vegetated by shrubs or cacti (Acacia?) is indicated by the rhizoliths found in the facies.

Trough cross-stratified conglomerate (Gt)

Description: The Gt facies is well exposed at Sili, Bhadarwa, Rayka and Phajalpur. The facies in the upper reaches occurs as isolated sediment bodies ranging in thickness between 1 m to 1.5 m (Profile 6.1-6.5). At places the facies occurs in association with Gp-facies. The lower bounding surface is erosive. The amplitude of trough ranges between 0.7 m to 1 m and are 3 m to 3.5 m wide. The foresets show normal grading and dip of 14° to 16° SW to SSW. The grading is well marked by coarse and fine bedding stratas. The clasts size ranges between 8 cm - 15 cm comprise dominantly quartzites, basalts and granite. The clasts are poorly sorted, well rounded and matrix supported.

In lower reaches the facies is better developed and shows lateral persistence (for more than 1 km). The facies occur are in the succession as 'ribbon like' bodies ranging in thickness between 0.5 to 3.5 m (Profile 6.1 and 6.2). The facies thickness decreases laterally on the either sides and merges with the horizontally stratified fine sand facies. The lower bounding surface is erosive with respect to the underlying mottled mud horizon. The amplitude of the trough varies between 1.5 m to 3.5 m and are 1.5 m to

20 m wide. The foresets are normal graded and dip at an angle of 18°-19° due SSE-SSW. The grading is marked by coarse and fine beds. The coarser beds range in thickness between 12 cm - 15 cm, comprises mainly carbonate clasts ranging in size between 15 cm - 18 cm in diameter alongwith some basaltic clasts. While the finer beds (coarse sand) are of 6 cm - 8 cm thick, comprises clasts size of 1 cm - 1.5 cm in diameter. The center portion of the troughs are marked by clustering of carbonate clasts. The facies shows embedded aggregates of mud clasts (25 cm - 50 cm) within the 20 m wide mega-troughs. Smaller troughs of 1.5 m - 2 m in width are also noticed. Generally the magnitude of the trough decreases upward within each unit and is observed that the sediment shows planar cross-stratification at the top of the storey. At places the foresets show tangential contact. The wedge like geometry is seen in this facies, here the bedding planes of the gravel and sand in which it occurs extend into the sand facies to form large troughs. One instance the facies show well developed epsilon cross-beds, with relatively high angle dip of foresets ranging between 18°-22° due ENE. This macroform extend laterally for a distance of about 75 m to 90 m.

Microscopic studies reveals that trough cross-stratified conglomerate comprises dominant calcrete nodules in their clast composition and a variety of framework grains with abundant interstitial carbonate cement/sparry cement. The grains mainly consists of quartz, feldspars, calcite and rock fragments (of quartzite, granite and basalt etc.). It is classified as polymictic conglomerate (Pettijohn, 1968).

The matrix is coarse grained and comprises two varieties of quartz - monocrystalline and polycrystalline quartz, feldspars - plagioclase, orthoclase and microcline, and rock fragments of quartzite, basalt, granite etc. These detrital clasts and minerals are embedded within the groundmass occurring both as sparry and micritic cementing material. The spar cement fills the intergranular space and micrite cement has been observed as enveloping the grain margins. The polycrystalline quartz occurs as sub-angular to sub-rounded grains embedded within the sparry/calcite cement. These grains show sutured boundaries between the crystals. The sub-rounded quartzite grains are also observed (Plate 6.6). Feldspars of both the varieties, the potash feldspars (mainly orthoclase and microcline) and sodic feldspars (mainly plagioclase) have been observed. The plagioclase feldspars show typical multiple twinning, concretion along the margins by micritic material and groundmass comprises smaller monocrystalline quartz and calcite grains. The microcline grains are sub-angular to sub-rounded in shape. The grains are unaltered and show well developed typical cross-hatched twinning (Plate 6.7). The calcrete nodules are abundant and are sub-rounded to rounded (Plate 6.8), and does not show any nucleus. The nodules comprise micro-crystalline carbonate with angular to sub-angular grains of quartz. The cracks in the nodules are filled by microspar cement and some grains show coating of micrite.

Interpretation: The facies was formed by the downstream migration of trains of mega sinuous crested dunes (Miall, 1978; Todd and Went, 1985; Billi *et al.*, 1987; Todd and Went, 1991) in a deepest part of the channel. The change in foreset dips from high (16°-18°) passing into almost horizontally bedded conglomerate bed suggests deposition near the transition to upper stage plane beds (Smith, 1990). The merging nature of the facies on either side into overbank facies suggests the channel

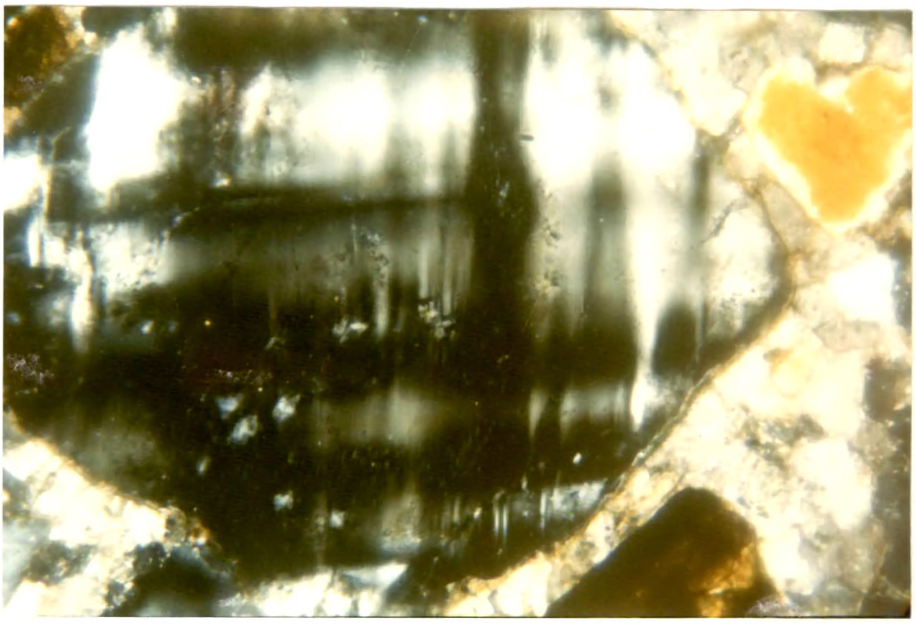

0 1 mm.

Plate 6.7 : Photomicrograph showing cross-hatched microcline sorrounded by sparry cement. (X-Nicols)

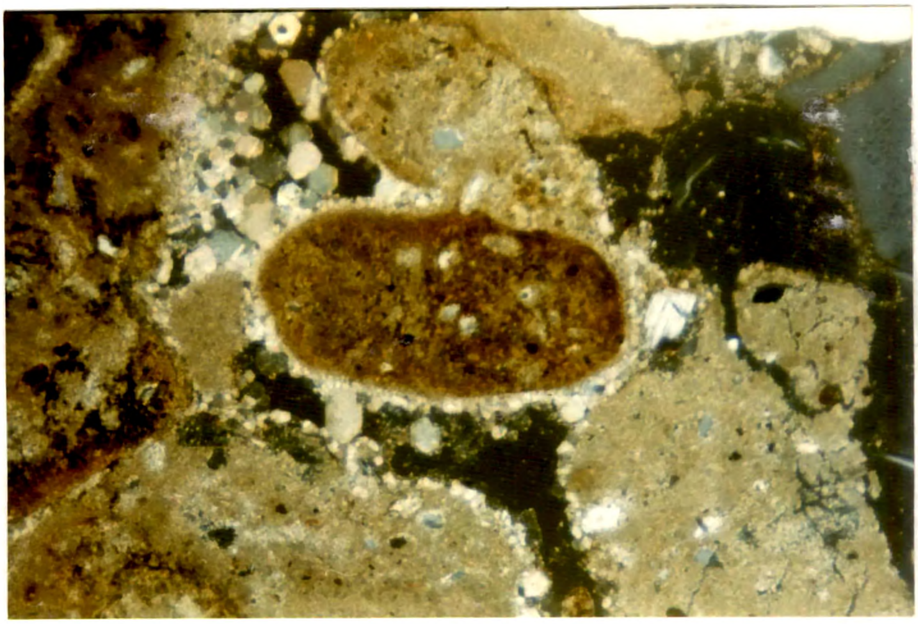

0 0.25 mm.

Plate 6.8 : Photomicrograph showing sub-rounded to rounded carbonate nodules. (X-Nicols)

margins. The maximum thickness of 3 m - 3.5 m suggests flow depth of a similar magnitude. The change in trough dimension indicates fluctuating flow regime. The large troughs of >20 m in width represents the minor channel fills (Miall, 1985). The presence of huge mud clasts indicates high energy flow condition. Epsilon beds are indicative of lateral accretion (LA) of macroform probably a longitudinal bar in a low sinuosity channel (Miall, 1985; 1986; 1988a). The accretion direction in ENE suggest reactivation of bounding surfaces that erode the previous deposited units. The wedge shaped geometry at the base of channel-fill represents deposition in a palaeo-thalweg where flow velocities were comparatively high. The thin section studies have revealed that the calcrete or carbonate nodules were derived from the alluvial plain and suggests short distance transport. Even the major mineral constituent occurring within the matrix viz. polycrystalline quartz, feldspars - plagioclase, orthoclase and microcline suggests near by granitic, basaltic and metamorphic source and short distance transport and the sutured boundaries in the polycrystalline quartz and occurrence of quartzitic fragments also suggests source from metamorphic rocks (Folk, 1968; Young, 1976; Adams *et al.*, 1986).

Massive silts (Sim)

Description: This facies occurs extensively in the Mahi river basin. It ranges in thickness from 2 m - 7 m and caps the fluvial sediment succession. In contrast to the irregular outcrop expression of the other facies, this facies forms steep vertical bluffs (Plate 5.4). This feature reflects the homogeneity in grain size. Geomorphologically, the facies occurs as mounds at some sites, while commonly it forms a ubiquitous sheet.

The facies is massive, structureless and is yellowish-brown in colour. Centimeter size carbonate nodules are distributed in this facies, and are more dense towards the top. The granulometric analysis of representative samples of this facies from different locations yield identical grain size distribution as seen in histogram, which shows unimodal nature (Fig. 6.3). The sediment shows mean grain size ranging between 3.8 Ø to 3.85 Ø, are moderately well sorted and contain on an average 58% to 64% of silts, 30% to 25% of sand and 12% to 11% of clay.

Interpretation: Based on grain size distribution characteristics along with homogeneity in the sediment size, ubiquity of this facies and absence of sedimentary structures it has been interpreted as having formed through aeolian agencies. These deposits in their geomorphological expression represent ancient dunal topography which has since been dissected by streams. Such dunal topography has also been recognized by Allchin and Goudie (1971) and a similar inference has been suggested. Pant and Chamyal (1990) term the deposits as being 'loess like', based on grain size characteristics and presence of vertical bluffs.

Horizontally laminated fine silty-sand (Fl)

Description: The facies is common in the sediment successions exposed between Kothiyakhad and Singrot that lies in the coastal zone (Plate 6.9). These comprise alternate parallel laminae of very fine silt and clay. The individual thickness of the laminae varies between 0.5 cm to 0.8 cm, while the thickness of the lithounits varies from 0.4 m to 0.5 m, comprising dominantly quartz sand alongwith mica flakes.

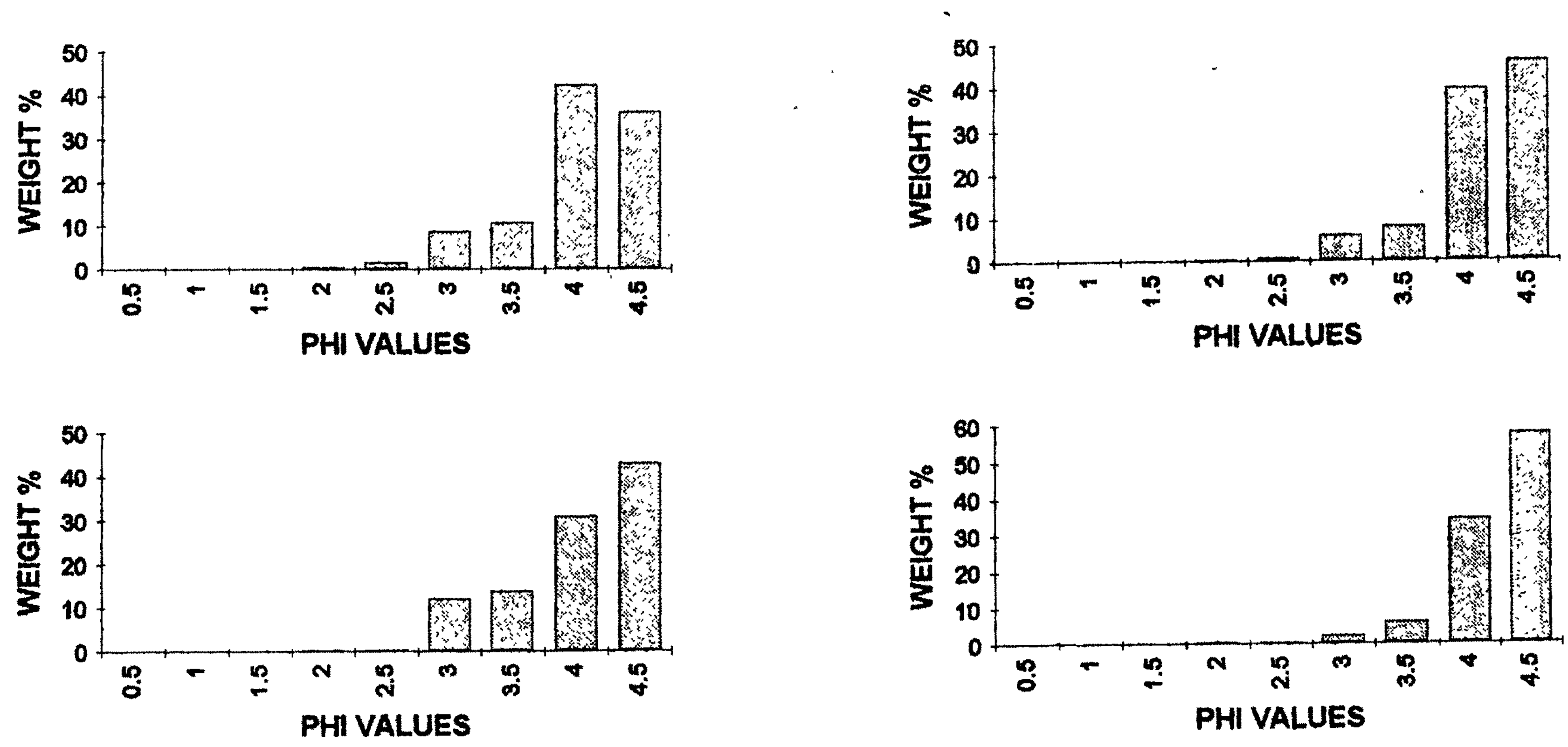

Fig. 6.3 : Representative histogram showing grain size distributions of the Sim facies

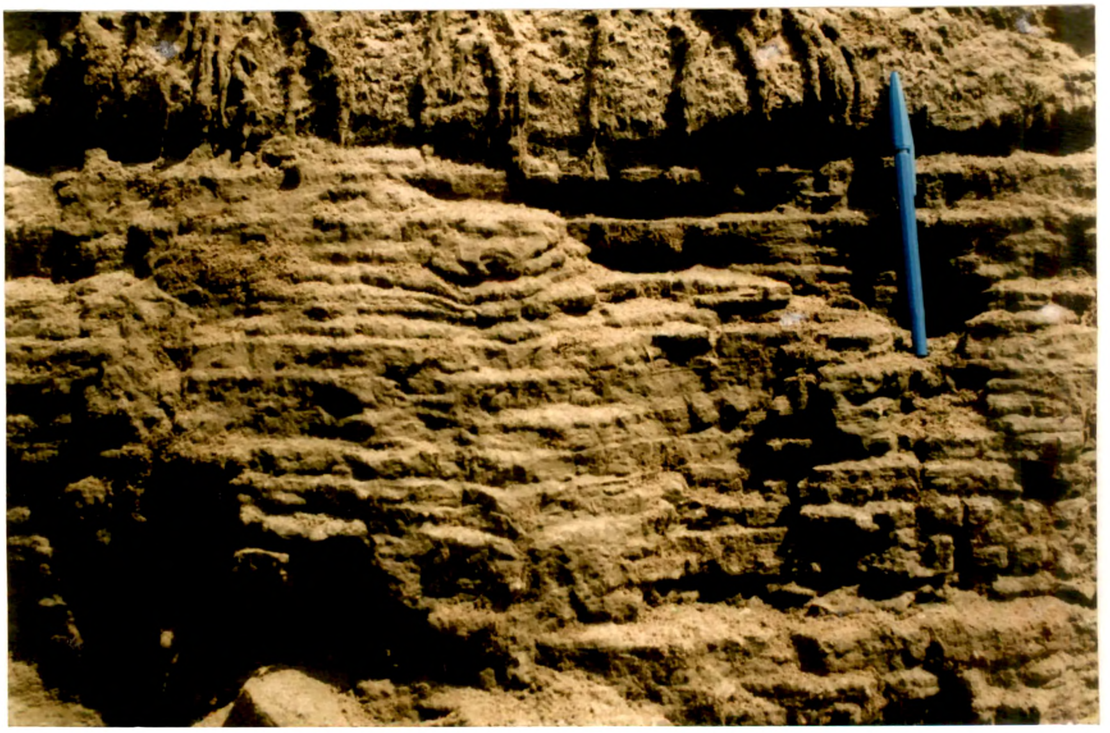

Plate 6.9 : Horizontally laminated silty-sand facies (Fl) at Kothiyakhad.

Plate 6.10 : Planar cross-stratified sand facies (Sp) showing herringbone structure at Kothiyakhad.

Laterally these extend for about 1 km to 1.5 km having transitional contacts with respect to the underlying mud horizon.

Interpretation: The parallel laminated Fl-facies was deposited under an estuarine environment and represent the tidal sand bar that formed within the broad funnel shaped estuarine mouth (Reading, 1986; Dalrymple *et al.*, 1992; Allen and Posamentier, 1993).

Planar cross-stratified sand (Sp)

Description: Planar cross-stratified facies is well exposed at Kothiyakhad laterally persistent for more than 0.5 km and vary in thickness between 0.75 m to 1 m. The internal beddings are well marked by the light and dark units of sand and silt. The sand comprises mainly quartz grains with mica flakes. The foresets show varying dip ranging between 26°-28° due NW-NNW. At places it shows well developed bi-directional structures - "Herringbone sets" (Plate 6.10). The planar cross-strata show mean palaeocurrent directions due 320° NNW and 135° SE. The foresets at places are draped by clay and interlaminated clay-silt laminaes. The ends of this unit are marked by highly inclined foresets ranging in dip between 32°-35°.

Interpretation: The facies typically suggests deposition under estuarine environment (Dalrymple, *et al.*, 1992). Presence of the herringbone structures are indicative of deposition under high energy condition developed during ebb-flood in a macrotidal funnel shaped estuary and the occurrence of clay drapes suggests bedform migration during tidal fluctuations (Reading, 1986).

Laminated mud facies (Fsc)

Description: This facies is well exposed between Kothiyakhad and Singrot. The thickness of the lithounit varies between 0.3 m - 0.5 m. The alternate laminas are marked by very fine silt and mud. The individual thickness of laminas ranges between 1.1 cm - 1.5 cm. The facies show well developed flaser bedding at the base which marks the contact between the underlying Fl-facies.

Interpretation: This laminated mud facies and well developed flasers within it are indicative of deposition in a tidal flat and marshes bordering the estuary (Reading, 1986; Dalrymple *et al.*, 1992 and Allen and Posamentier, 1993). The occurrence of this lithounit over the laminated sand suggests migration of minor tidal inlets/channels within the estuarine limits.

Palaeosols (P)

Interlayered palaeosols in the sediment record occur at several stratigraphic intervals. Of widespread occurrence are basal soils which show vertic features and a ubiquitous red-soil horizon which bisects the stratigraphic succession into two parts, above as aeolian and below as fluvial sediment succession.

Vertisol

Description: Commonly at two stratigraphic levels, there occur clays which show intense fracturing and forms the base of the coarse and fine grained overlying fluvial sediments. The horizon is well exposed in the lower reaches of Mahi basin between Bhadarwa and Mohommadpura and range in thickness from 0.5 m - >4 m (Pant and

Chamyal, 1990). The basal vertisol profile is well developed, but does not show any horizonization due to homogeneous fine sediments. The horizon shows light brown (10YR 5/4) to brown colour (7.5YR 5/4). This lithounit is intensely fractured, resulting into formation of blocks with planar faces. Intersection of these planar faces has given rise to sub-angular blocky nature. Along the ped faces well developed slickensides are also observed. At places the horizon is desiccated, which is well marked by vertical cracks/fissures, that were later filled by fine detrital sediments. These fissures presently occur as vertical calcrete pipes. The anticline folds or concave upward curvi-planes are also observed at some places. The fractured planes occur parallel to the limbs of the folds. The scattered nodules show sharp boundary (or disorthic nature) with the host sediments. Tubular forms of carbonate pipes (rhizocretions) are also common at some places which extend much below the zone of fracturing. Pedogenic features like burrows and extensive root modification marked by network of rhizoliths are well observed. The clay mineral assemblage is dominated by very high percentage of smectite (montmorillonite) with subordinate quantities of illite and kaolinite (Table 6.2). The high concentration of smectite (montmorillonite) shows relative peak value of 14.44 Å and 16.87 Å upon glycolation. Illite shows peak at 10.04 Å and 5.01 Å, whereas kaolinite shows 7.15 Å. Non-clay mineral like quartz was also identified at a peak value of 4.26 Å and 3.34 Å (Fig. 6.4, Table 6.2).

Interpretation: The homogenization of the soil profile and the presence of folds or concave-up curvi-planar joints suggest the soil to be of the vertisol type (Dudal and Eswaran, 1988; Gustavson, 1991; Marriott and Wright, 1993). This fold like

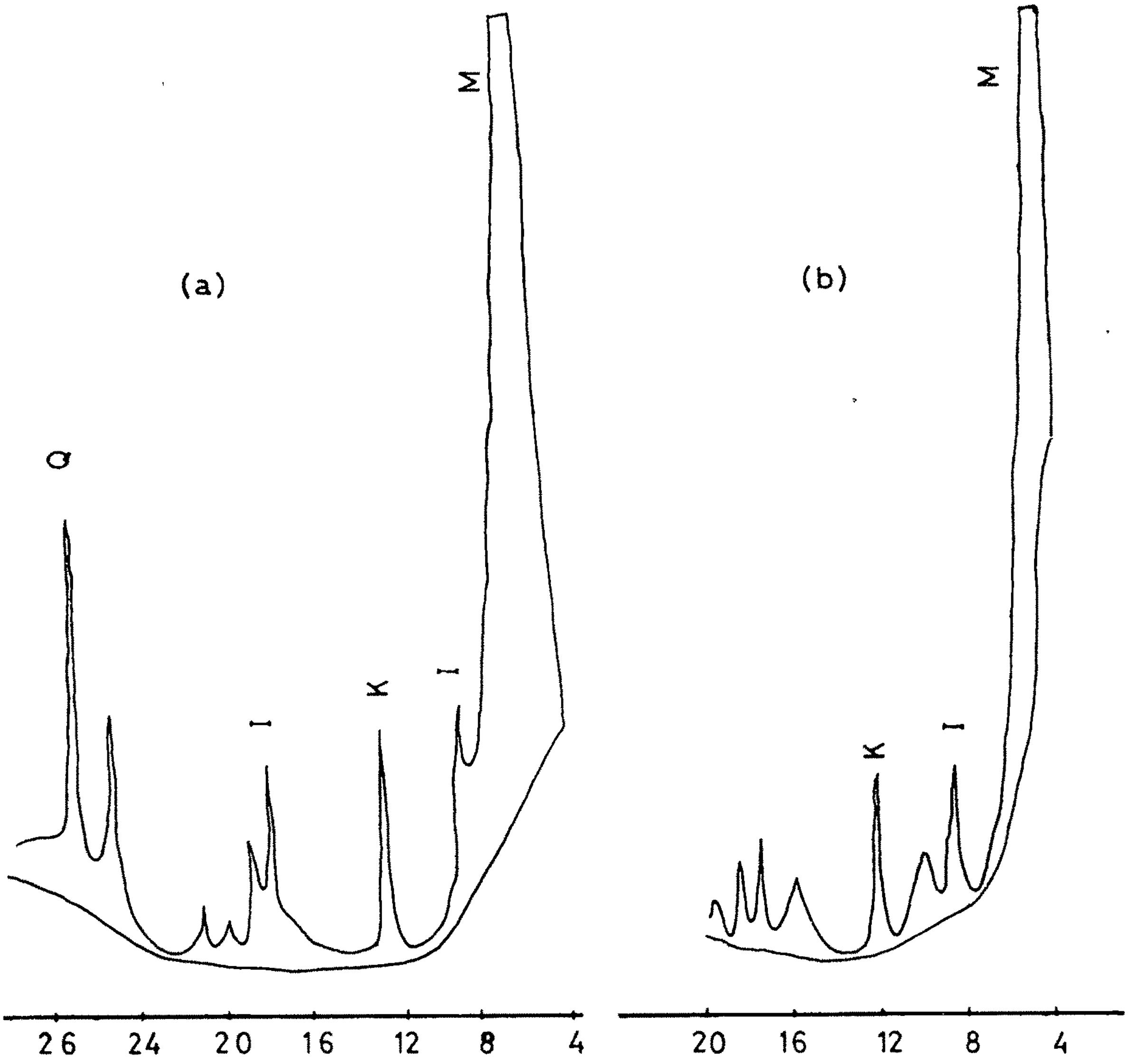

Fig. 6.4 : X-Ray diffractogram of clay fraction of vertisol facies
(a) Peaks of unglycoloated sample and (b) Enhanced peaks of montmorillonite/smectite after glycolation. M-montmorillonite, I-illite, K-kaolinite, Q-quartz

SOIL	MONTMORILLONITE	ILLITE	KAOLINITE	HEMATITE
VERTISOL	■ ■ ■ ■ ■	■ ■	■	
RED-SOIL	■ ■ ■ ■	■ ■ ■	■ ■	■
BROWN-SOIL	■ ■ ■ ■	■ ■	■ ■ ■	

■ ■ ■ ■ ■ 40% to 50%

■ ■ ■ ■ 30% to 40%

■ ■ ■ 20% to 30%

■ ■ 10% to 20%

■ 1% to 10%

Table 6.2 : Relative dominances of clay minerals calculated from the magnitude of the 001 peaks.

structures might have been formed due to development of deep vertical desiccation/cracks during the dry phases, which later during calcretization of the fine detrital sediments causes slight buckling upward of the adjacent stratas. The result of this deformation have lead to the extension of cracks that provided site for carbonate nodule formation (Watts, 1977). This suggests the alternate spells of wet and dry phases. Such features have also been described as pseudo-anticlines (Watts, 1977) (Plate 5.4). The disorthic nature of the carbonate nodules indicates frequent churning of the soil. Tubular forms of carbonates are remnants of root systems which formed through a complex process of circum-root precipitation and subsequent infilling and are interpreted as rhizoliths (Klappa, 1980; Jones and Ng, 1988). Movement within the soil is indicated by the slickensides which form during shrinking and swelling of the clays resulting in the formation of stress cutans (Wilding and Tessier, 1988). The high concentration of clay also suggests extensive weathering and pedoturbation activity. The shrinkage and swelling phenomenon was responsible for the formation of clay minerals, evidenced by the dominance of montmorillonite, it supports the contention that the soil was susceptible to large scale shrinking and swelling, since in the vertisols the world over clay mineral assemblages are dominated by this particular group and today the vertisol generally forms in an area experiencing a seasonal rainfall with about 4-5 wet months where the rainfall varies between 500 to 1200 mm (Dudal and Eswaran, 1988; Coulombe *et al.*, 1996).

Red-soil

Description: The soil is yellowish red in colour (5YR 5/6), and ranges in thickness from ~1 m to 3 m. This lithounit is well exposed between Shihora to Kavi. The upper surface of the unit is irregular and undulatory exhibiting shallow mounds and depressions at a continuous exposure at Dabka (Plate 5.9). The red unit is fractured by multiple set of joints due to which develop subangular blocky aggregates. The surfaces of such aggregates shows occurrence of clay films. The degree of cementation by carbonate varies progressively southwards. In the southern sections (near Dabka) the cementation is so high that hammer blows have no effect on the unit. This soil profile has well developed Bk and C horizon, where as O and A horizons are absent. The Bk horizon occurs at a variable depth in the profile exposed at different locations. The depth varies between 0.45 m to 5 m from the top. The Bk horizon shows high concentration of carbonate nodules, and comprises finer sediments suggesting accumulation of illuviated clays. The carbonate nodules show sharp margins with the host sediments and ranges in size between 1.5 cm - 3 cm. The underlying C horizon shows slightly coarser sediment size and scattered occurrence of carbonate nodules. The granulometric analysis of this red soil lithofacies show mean average grain size ranging between 3.45 Ø - 3.75 Ø. The histograms of this lithounit show bimodal nature (Fig. 6.5), the prominent values ranging between 2.5 Ø - 4.5 Ø. The sediments are composed of 54% to 74% sand, 28% to 20% silt and 18% to 6% of clay. The sediments are moderately to moderately well sorted. The clay mineral assemblage is dominated by smectite (montmorillonite) with subordinate amount of illite, kaolinite

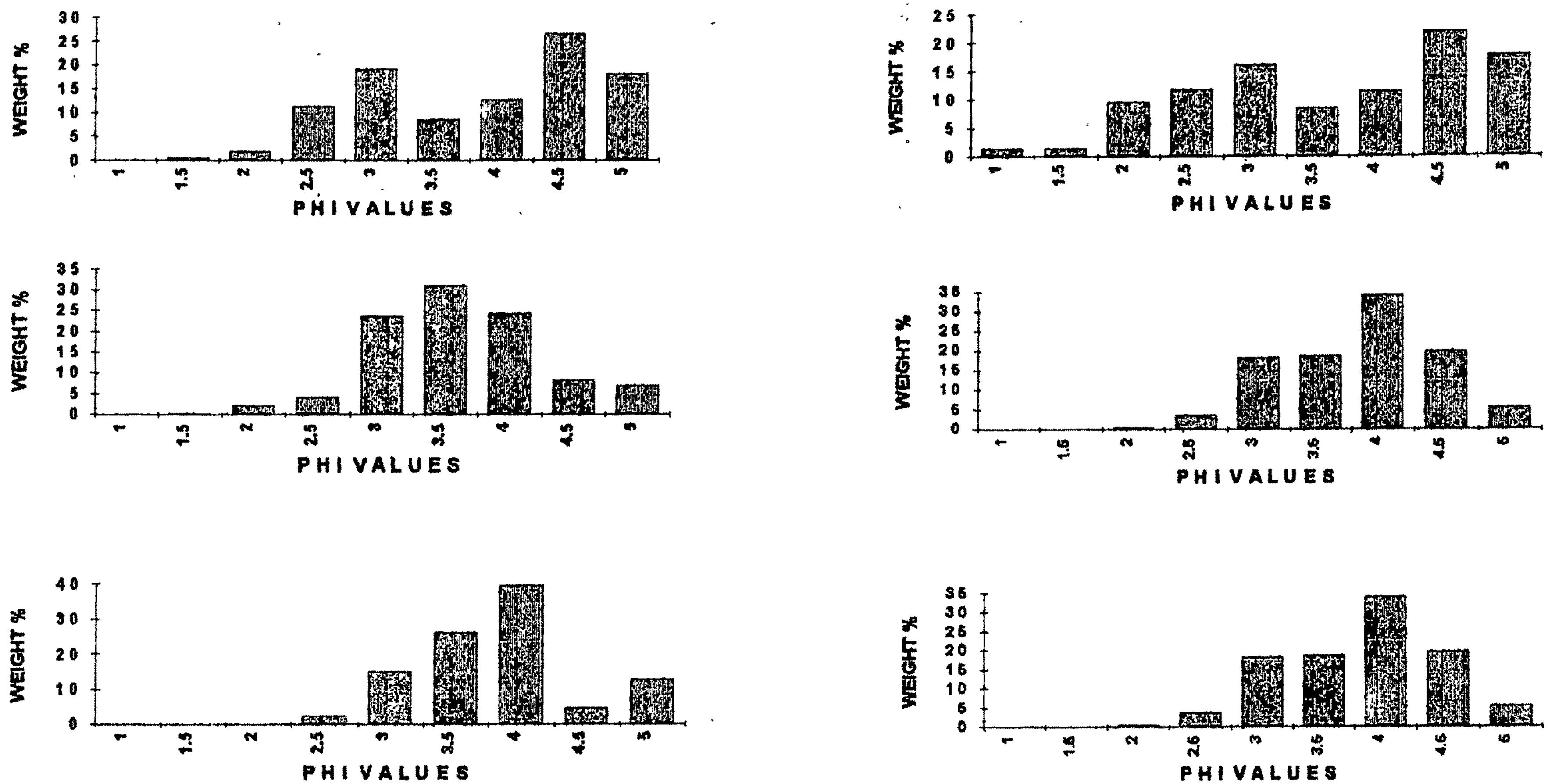

Fig. 6.5 : Representative histogram showing grain size distribution of the Red Soil facies

and traceable amount of hematite (Fig. 6.6, Table 6.2). The non-clay minerals like quartz and calcite are also present. The smectite (montmorillonite) shows relative peak intensities ranging between 13.7 Å - 14.23 Å and enhanced peak at 16.9 Å upon glycolation. The kaolinite shows relative peaks at 7.07 Å - 7.19 Å - 4.55 Å - 3.59 Å and 3.56 Å. The illite show 10.03 Å - 9.98 Å - 4.98 Å, hematite is observed in trace amounts only at 3.66 Å. Whereas the non-clay minerals viz. calcite and quartz were identified at 3.03 Å and 3.34 Å.

Interpretation: On the basis of the granulometric analysis this soil horizon can be categorized as sandy loam (Birkeland, 1984). The undulatory nature of the upper contact suggests a subdued palaeotopography or uneven floodplain topography. Absence of 'A'-horizon suggests that it must have been eroded during the period of non-deposition or by the subsequent depositional event. The well developed Bk-horizon and pedogenic features suggests strongly developed soil profile (Birkeland, 1984). Pedogenesis is indicated by clay translocation along ped faces which is well marked by high concentration of finer sediments in the Bk-horizon. The higher degree of cementation in the southern sections suggest proximity of the coast. Carbonate rich sea sprays are thought to have been responsible for the relative hardness of red-soil sections as compared to profiles studied at northern sites. The high concentration of smectite (montomorillonite) alongwith subordinate amount of illite, kaolinite and hematite (in trace amounts) suggests that the parent sediments from which these clay minerals formed were rich in ferromagnesium minerals, alongwith potash and sodic feldspars and micas (Pye, 1983; Birkeland, 1984; Singer, 1984; Weaver, 1989). The

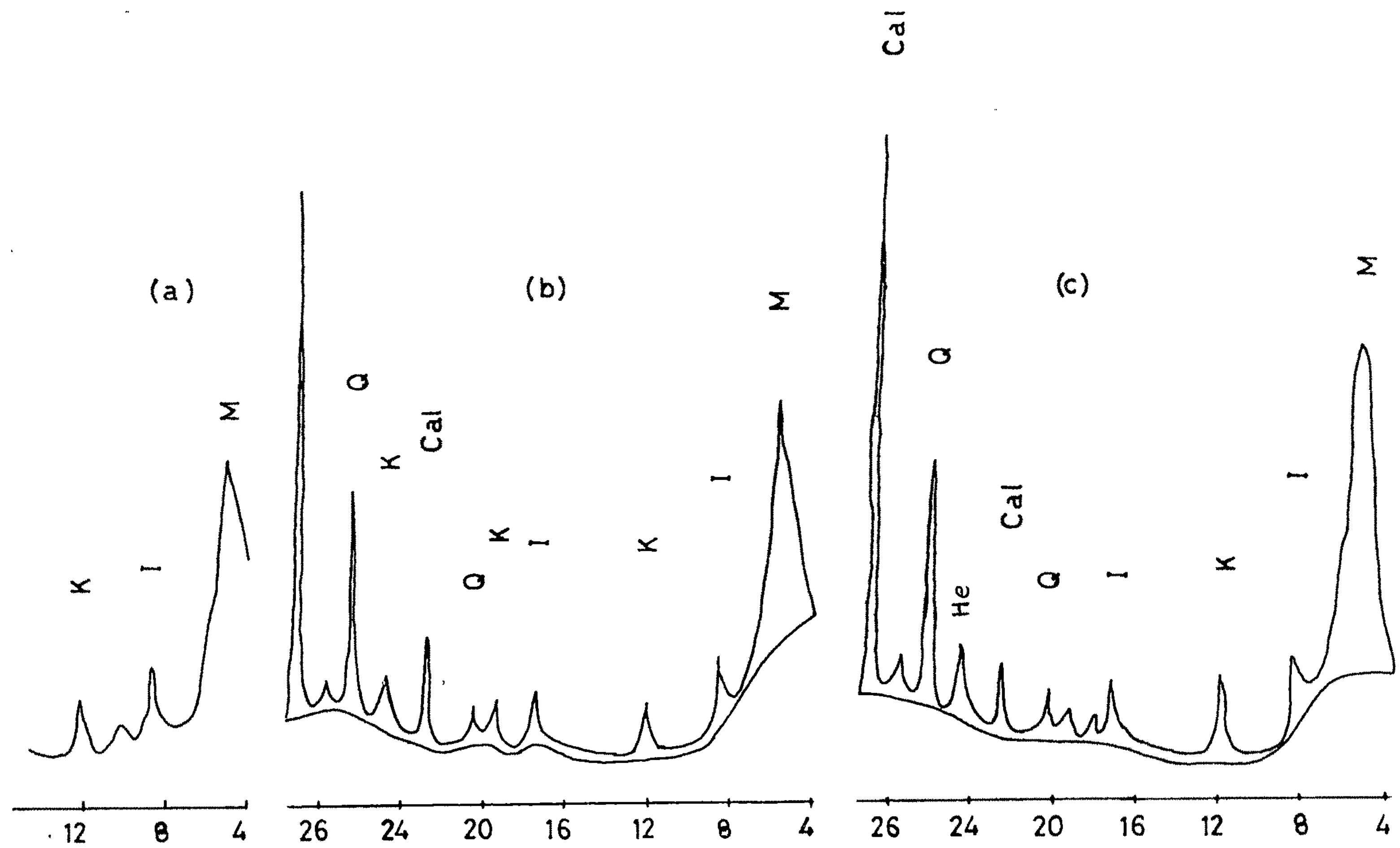

Fig. 6.6 : X-Ray diffractogram of clay fractions of Red Soil facies
(a,c) Peaks of unglycolated sample and (b) Enhancement of montmorillonite/smectite peak after glycolation. M-montmorillonite, I-illite, K-kaolinite, Q-quartz, Cal-calcite, He-Hematite.

presence of montmorillonite suggests poor leaching conditions (Birkeland 1984; Weaver, 1989). This is in accordance with the basalt granules found in the host sediments, the weathering of which led to the above mentioned neoformed clays mainly smectite (montmorillonite). It is also suggested that the sediments comprising the ferromagnesium mineral must have released iron compounds during the process of hydrolysis in relatively humid or sub-humid climate and during the subsequent dry period (dehydration) resulted in the formation of hematite in trace amounts (Birkeland, 1984). The apparent presence of hematite in trace amounts may be because of lack of crystallinity of the mineral (Pye, 1983). Hematite appears to be the mineral responsible for the red colouration of the soil horizon (Pye, 1983). The clay mineralogy suggests that the sediments were derived from granitic, basaltic and metamorphic terrains. The presence of carbonate nodules at the lower portions of the profile suggests that these are related to the weathering processes. The palaeo-precipitation values calculated using the equation given by Retallack (1995) gives values of around 2000 mm for a depth of 350 cm. Since this is unlikely it is suggested that the red-soil is actually a pedo-complex and spans a considerable amount of time.

Brown soil

Description: Two buried soils show yellowish brown (10YR 5/4) and very pale brown colours (10YR 7/4) (Plate 5.11). These lithounits are exposed almost all along the cliffs in the Mahi valley. The upper contact of the soil is sharp and undulatory. The thickness of the horizons is 3 m. The soil is of blocky nature and shows well developed aggregates, surfaces of which show clay films. The soil profiles does not show well developed Bk and C horizons. Small sub-millimeter diameter buried root channels are seen which are lined by black coloured carbon. These soils at places are less calcified compared to the overlying rubified soil unit. Carbonate nodules are present which are orthic and irregular in morphology. The nodules are on an average 1 cm - 2 cm in size. The granulometric analysis of these soil facies show mean average grain size ranging between 3.33 Ø - 3.96 Ø. The histograms show bimodal nature, ranging between 3 Ø - 5 Ø (Fig. 6.7). The sediment shows average percentages of sand 48% to 62%; 36% to 28% of silts and 16% to 8% of clay. The sediments are moderate to moderately well sorted. The clay mineral assemblage shows high concentration of montmorillonite alongwith subordinate amount of kaolinite and illite (Table 6.2). The montmorillonite is identified by relative peak at 14.67 Å - 14.14 Å. The next dominant clay mineral is kaolinite which shows peaks at 7.14 Å - 7.13 Å and repeated peaks at 3.57 Å - 3.56 Å - 3.59 Å. The illite shows 9.98 Å - 10.03 Å - 10.06 Å and repeated peak at 4.98 Å - 4.99 Å - 4.99 Å. The fine detrital minerals identified were viz. quartz showing 3.33 Å - 3.35 Å and calcite at 3.22 Å in trace amount (Fig. 6.8).

Interpretation: On the basis of the granulometric data these soils can be categorized as sandy loam, and the absence of well developed Bk and C horizon suggests that these soil profiles are moderate to weakly developed soils (Birkeland, 1984). These brown coloured horizons at places show evidences of soil formation in the form of clay illuviation, presence of root channels, development of aggregates (peds) and calcrete nodules. The clay mineral assemblage shows dominance of montmorillonite alongwith subordinate kaolinite and illite. This suggest that the detritus are rich in feldspar

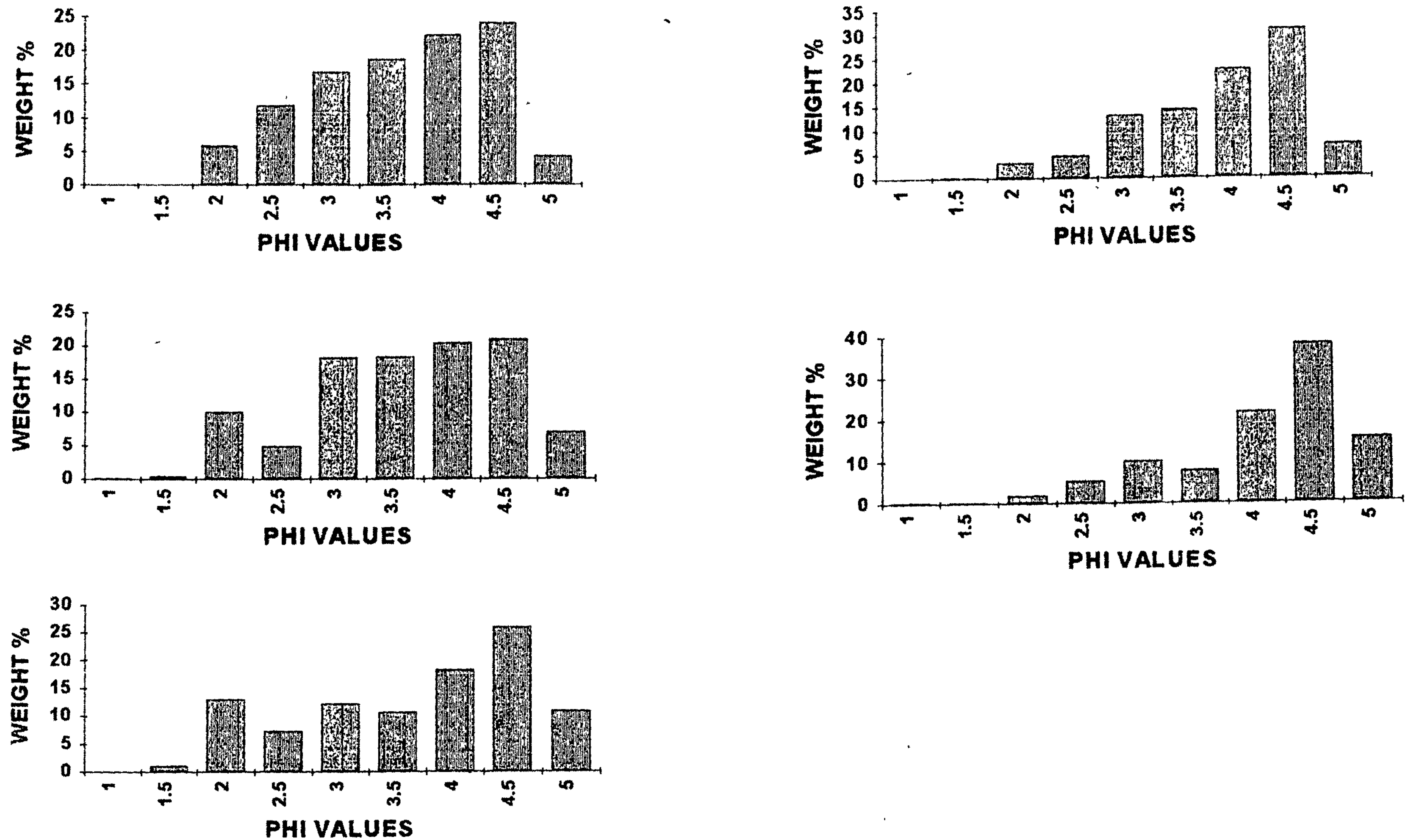

Fig. 6.7a : Representative histogram showing grain size distribution of the Brown Soil -1 facies

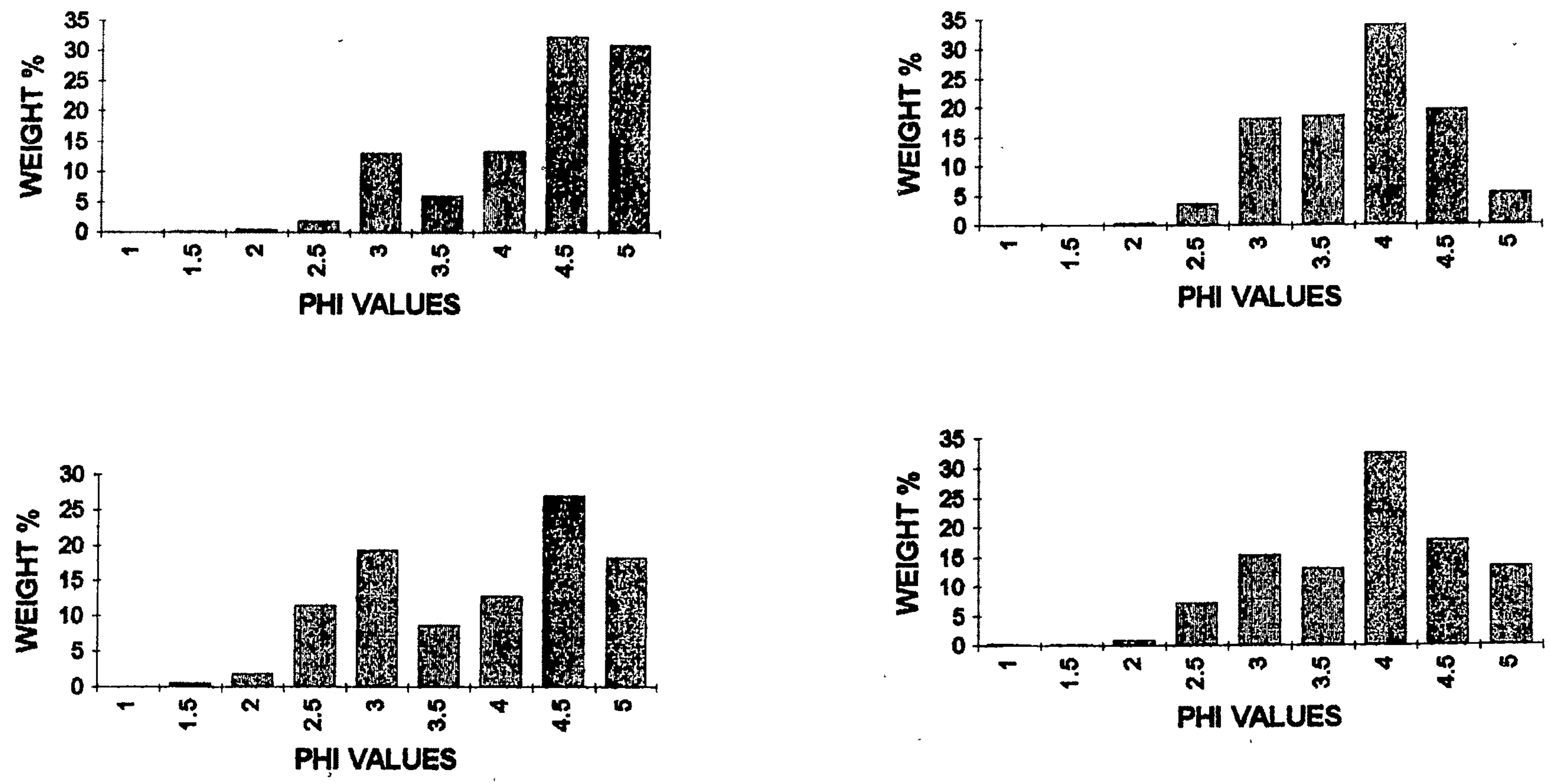

Fig. 6.7b : Representative histograms showing grain size distribution of the Brown Soil - 2 facies

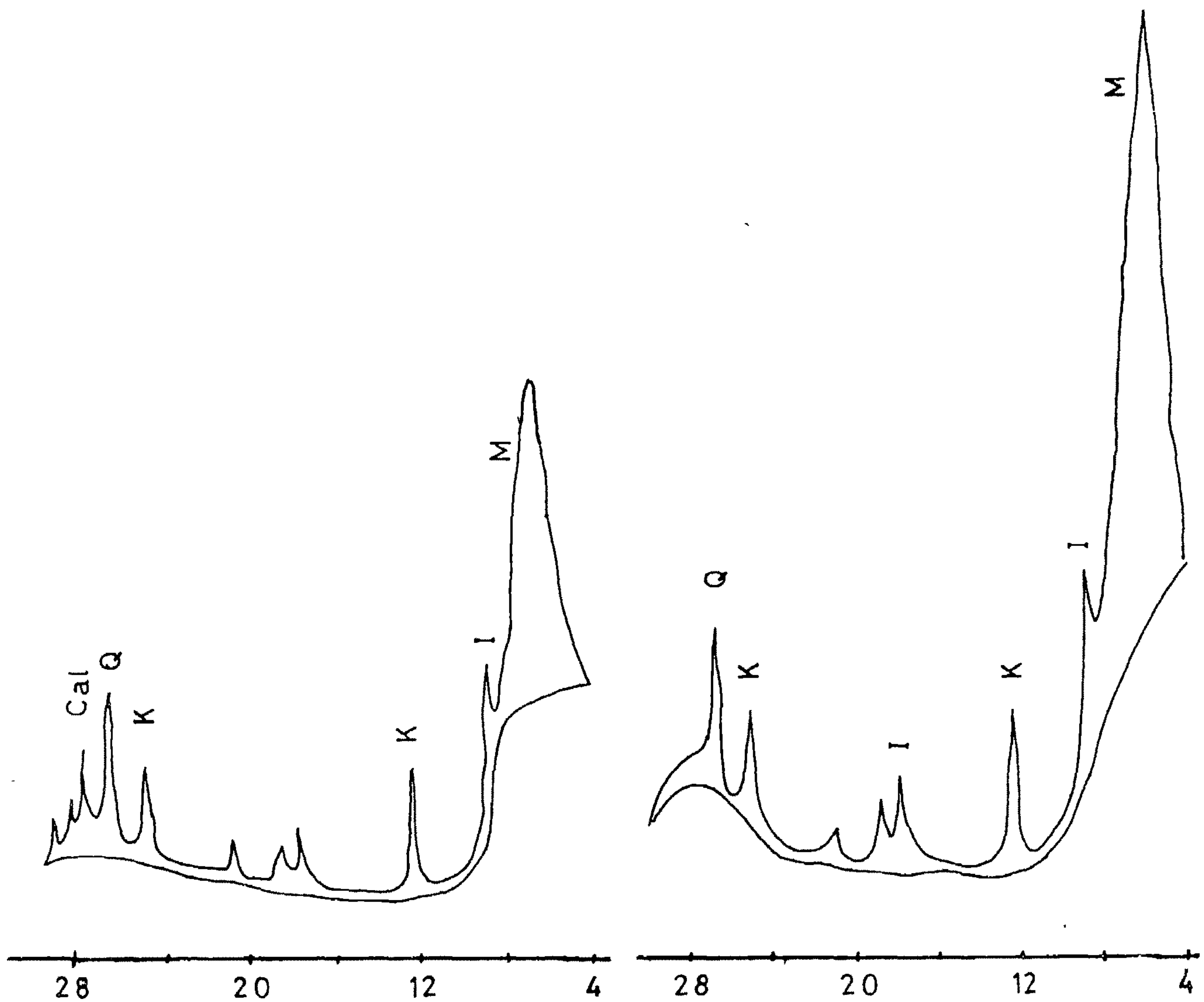

Fig. 6.8a : X-Ray diffractogram of clay fraction of Brown Soil - I facies.
M-montmorillonite, I-illite, K-kaolinite, Q-quartz, Cal-calcite.

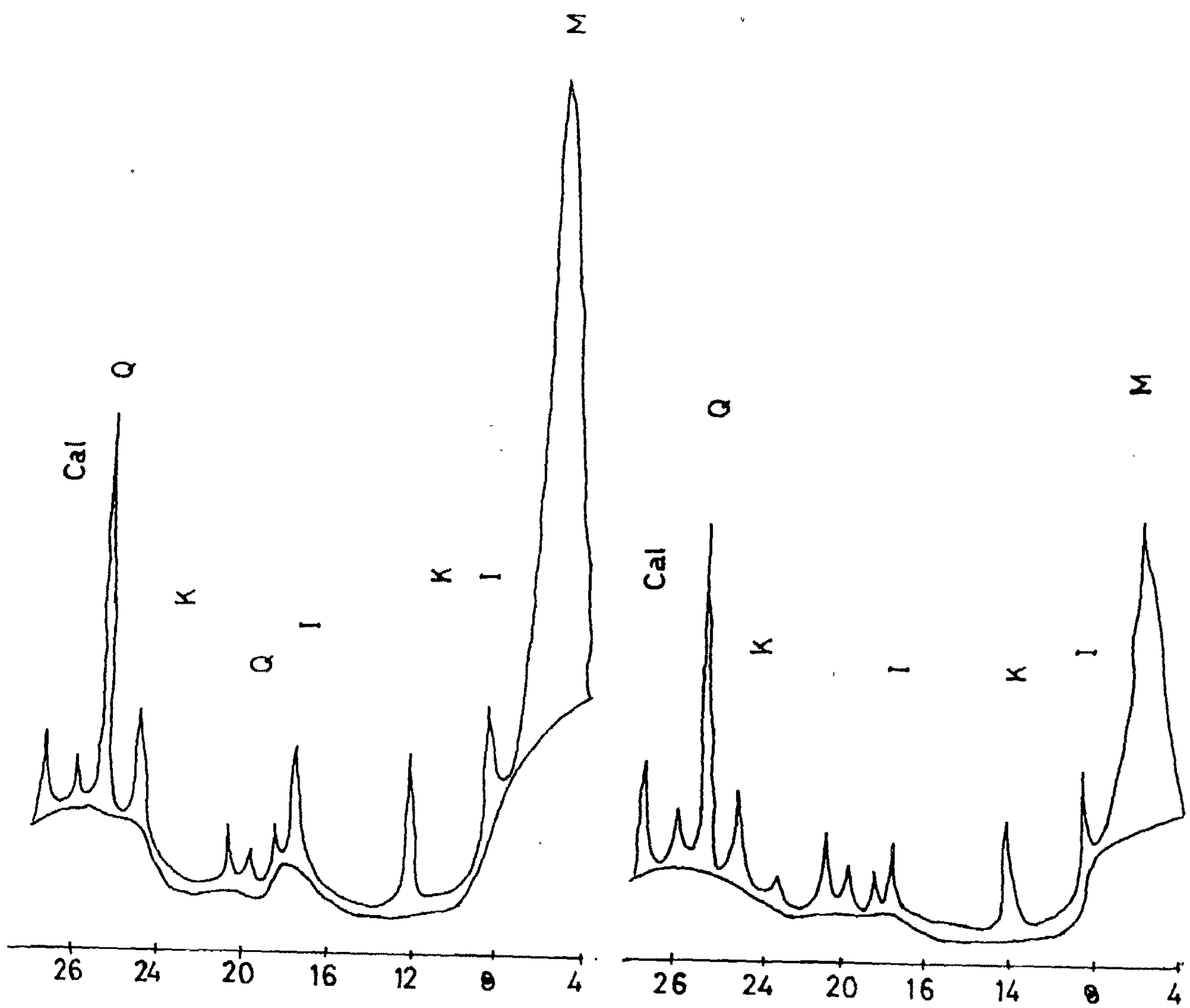

Fig. 6.8b : X-Ray diffractogram of clay fraction of Brown Soil - II facies.
M-montmorillonite, I-illite, K-kaolinite, Q-quartz, Cal-calcite.

mainly plagioclase and orthoclase alongwith some micaceous minerals derived from granitic and metamorphic terrains. The presence of kaolinite indicates wetter climates having precipitation of >900 mm (Weaver, 1989). Kaolinite forms in conditions of high leaching and the contrasting presence of calcareous glaebules (though less profuse) may be attributed to drier time spans. The brown colour of the soil may probably be due to the presence of goethite (Pye, 1983), although it has not been possible to identify it in the XRD analyses.

BOUNDING SURFACES IN THE FLUVIAL SEDIMENT PROFILES

The large scale photomosaics were used to study lateral profiles. Best exposed 2-dimension outcrops in the lower Mahi basin around Rayka and Phajalpur were considered for detailed studies. Total six lateral profiles were studied. The first step in describing these profiles was to recognize the major bounding surfaces (Allen, 1983) that bound the major bedforms and for (i) sub-division of succession into its constituent lithofacies assemblages, and (ii) identification of mesoforms and macroforms. This study has helped in describing the abundant and lateral facies changes.

The bounding surfaces were defined on the basis of revised classification of six types of bounding surfaces of Miall (1988a). According to Miall (1988a) even in the excellent outcrops the correct classification of bounding surfaces is not always easy, but suggested following three useful rules that makes the identification easier.

1) A surface of any given order may be truncated by a surface of equal or higher order, but not by one of lower order.

2) As bounding surfaces mainly record erosional events, they must be defined on the basis of what follows them rather than what precedes them e.g. the top of the macroform is defined by a 4th order surface, except where it has been cut into by a major channel, the base of which typically constitutes a 5th order surface.

3) Other minor surfaces may change rank laterally, e.g. the upper 4th order surface of macroform may merge into a 2nd order surface in the floor of an adjacent channel.

The bounding surfaces identified in the Mahi basin are summarized below:

Order of bounding surfaces	Description of bounding surfaces
First order	Set of bounding surfaces with little or no internal erosion.
Second order	Coset-bounding surfaces, associated with a change of lithofacies types, does not show significant truncation.
Third order	Cross-cutting erosional surfaces which dips at low angle, marks the lateral accretion (LA) and downstream accretion (DA) element of macroform and are bounded by higher 4th order, i.e. they record increments of macroform accretion.
Fourth order	Flat to convex-up bounding surface representing the upper bounding surface of macroform, also represent lateral accretion (LA) and downstream accretion (DA) of macroform. They are also defined as the basal scour surface of minor channels.
Fifth order	Flat to slightly concave-up bounding surface, they are laterally extensive, represent the lower bounding surface of major channel-fill complexes.

Of the six profiles studied, 1 and 2 were used to identify the lateral facies variation and lateral persistence of the individual lithounits. Interpretative line drawings sketch's of these profiles were prepared from the photo-mosaics (Profiles 6.1-6.6). The profiles show two higher order bounding surfaces which bound the storey of Gt and St lithounits. These two major surfaces are 5th and 4th order surfaces. The 5th order surfaces mark the base of macroforms consisting mainly Gt and St lithounits evidenced by the erosional contact, and run parallel to outcrop for about 250 m - 300 m. The 4th order surfaces represent the upper bounding surface of macroform (mainly Gt-lithounit), are flat to convex upward and also run parallel to the outcrop.

Profile-1. This profile is oriented N235° (Profile 6.1). It exhibits storeys of three major lithounits Gt, St and Sh. The two higher order surfaces 5th and 4th bound the macroforms. The 5th order surfaces bound the basal surface of St, which at places shows scouring nature with respect to their underlying lithounits. The 5th bounds at places the basal surface that shows scouring with respect to the underlying vertisol unit. The 3rd order surfaces mark the medium size troughs 2 m - 2.5 m in Gt-lithounit that truncates the lower 2nd and 1st order surfaces. At places in Gt facies the troughs are truncated by the succeeding troughs marked by 3rd order surfaces. The contact between the Gt and underlying St is marked by another 4th order surface that at places shows erosive nature. The underlying St lithounit shows shallow troughs of around 1 m - 1.5 m and about 30 m - 42 m wide. These troughs of St lithounit truncate the lower order surfaces of underlying Sh_1 lithounit. This Sh_1 lithounit shows well developed parallel horizontal bands of calcrete. The profile shows the storey of two trough cross-stratified facies (St and Gt). This facies marks the macroforms that represents shallow channel depth comparable with amplitudes of troughs. The palaeocurrent data show SSE direction of the channel. The truncation of troughs in both St and Gt lithounit suggests reactivation of 3rd order surface.

The pinching out nature of sand trough of about 30 m - 42 m in width and 1 m - 1.5 m amplitude suggests shallow channels that had flowed due SSE. These shallow channel margins are well evidenced by the increasing inclination of cross-beds on either sides of the trough. Since evidences of channel cutting are rare, it can be deduced that the channel avulsion was gradual and deposition took place under lower flow regime. The overlying Gt-facies suggests sudden increase in flow regime indicated by coarser bedload (calcrete clasts) and several aggregates of 0.5 m diameter mud clasts.

Profile-2. This profile shows the extension of the lithounits (Profile 6.2). In the right of the profile the Gt-lithounit almost pinches out and merges with the adjacent Sh_1-lithounits, that are bounded by lower order bounding surfaces. The left side of the profile shows 3rd order surfaces that truncates the underlying lower order surfaces of Sh_1-lithounits. The 4th order surfaces represents the epsilon cross-beds (left side of profile) dipping at higher angle than the foresets of trough and show uneven stratification.

The profile show ribbon like appearance bounded by 4th and 5th order surfaces. The merging of the Gt and St lithounits indicates channel margins. The epsilon cross-bedding represents lateral accretion of barform (Miall, 1988a, 1988b; Gibling and

Rust, 1990) in a channel that flowed due SSE. The uneven stratification of these cross-beds suggests accretion was highly episodic (Gibling and Rust, 1990). The detail studies of individual mesoforms and macroforms are described in profiles 3, 4, 5 and 6.

Profile-3. This profile is located in the upstream part in relation with the profile-1. The cliff section of profile is oriented N 205° parallel to the present day SSW flowing channel. Small to medium scale sedimentary are not visible at the scale of the photograph. Five bounding surfaces were identified in this profile (Profile 6.3). The section shows two lithofacies Gt and Sh_l alongwith the vertisol unit occurring between these two. The 5th order surfaces form the base of the extensively occurring Gt-lithounits which show slightly concave upward erosive nature, cutting at places the underlying 1st order surfaces of Sh_l-lithounit and vertisol unit. The thickness of the Gt unit in the left decreases upto almost 0.5 m and merges into the Sh_l overbank facies, while towards right (in downstream) the unit shows thickness of 3.5 m. The 4th order surface marks the upper portion of the Gt-lithounit, it is flat to convex upward. This 4th order surface separates the overlying Sh_l-lithounit. The gravelly lithounit comprise 3rd order surfaces that truncates the lower order foresets. The 2nd order surfaces is noticed in the upper portion of this lithounit where it bounds 1st order surfaces showing planar cross-stratification and dips of around 15°-16° due SE. The overlying and underlying horizontally stratified sand (Sh_l) lithofacies shows no internal erosion within the horizontal stratas of calcrete bands that are bounded by 1st order surfaces.

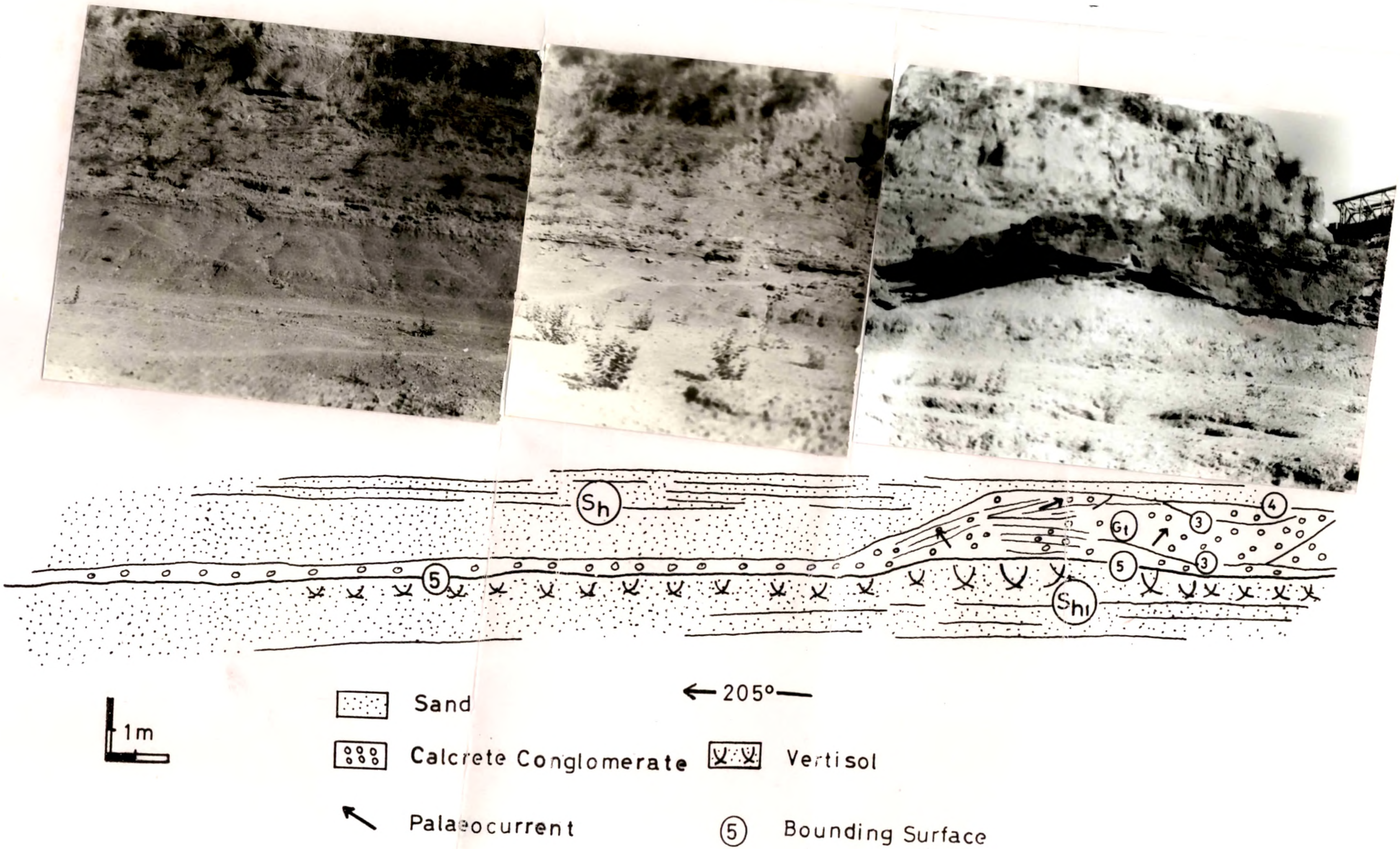
Sh
Gt
3
4
5
Shl
← 205° —
1m
Sand
Calcrete Conglomerate
Vertisol
Palaeocurrent
5
Bounding Surface

From this it can be said that the variable thickness of the Gt-lithounit between 0.5 m to 3.5 m, suggests that the 0.5 m thick unit and its merging nature with the Sh_1-lithofacies represents the channel margin and sudden increasing thickness of 3.5 m represents the palaeo-flow depth of the channel in which sedimentation took place. The erosive nature of 2nd order surfaces marks the minor changes in flow conditions (Allen, 1983; Miall, 1988a).

Profile-4. This profile lies adjacent to the profile-3 in downstream and shows extension of the same major lithofacies (Profile 6.4). The section shows Gt-lithofacies bounded by 5th order bounding surface at the base, while the top is bounded by 4th order surface. The internal lower order surfaces are 3rd order. The major trough of about 3.5 m in amplitude and is around 20 m wide are bounded by higher 5th order surface, that truncates the lower 2nd and 1st order surfaces that bounds almost planar stratified gravel in the right as well as the underlying vertisol unit. The 2nd order surfaces are also observed that marks change in lithofacies from calcrete conglomerate (Gt) to underlying sandy trough (St) facies.

The mega-troughs of 20 m wide and amplitude of 3.5 m bounded by 5th order surfaces suggests reactivation of the macroform indicated by channel scours. The minor troughs of about 1 m amplitude and 4 m width bounded by 3rd order surfaces suggests downstream migration of trains of sinuous crested dunes in the deepest part of the channel (Miall, 1978, 1985; Billi *et al.*, 1987; Miall 1988a, 1988b; Todd and Went, 1991). The change flow regime from low to high is marked by the presence of 2nd order surfaces (Miall, 1988a).

Profile-5. This profile forms a part of profile-2. It is oriented N 245°. The profile comprises 3 major lithofacies Gt, Sh_l, St (Profile 6.5). Here three bounding surfaces were identified. The 5th order surface bounds the base of the macroform comprising Gt and St - lithounits, while the top is bounded by the 4th order surface. The Gt-facies shows well developed epsilon cross-beds capped by 4th order surface alongwith internal 3rd lower order surfaces occurring parallel to it. The unit consists dominantly of coarse calcrete gravel clasts. The epsilon cross-beds show dip ranging between 19°-20° which is slightly higher than the dip's of trough foresets. They show dip in due N 75°E. To the right multiple storey troughs are seen marked by 3rd order that cuts the adjacent lower order surfaces. The macroform show lateral extent of about 25 m - 27 m. The sandy trough (St) show scouring with respect to the underlying Sh_l facies.

The epsilon cross-beds migrating in N 75°E suggests lateral accretion (LA) of the macroform (Miall, 1986). The palaeoflow of the channel in which this migration took place flowed due SSE-SSW. This lateral accreted macroform suggests migration or accretion of a channel-bar (Miall, 1986, 1988a, 1988b; Gibling and Rust, 1990).

Profile-6. This profile comprises Sh_l-lithofacies (Profile 6.6). It is oriented N 225°. Two higher order bounding surfaces. The 4th order surface marks the top of the lithounit and the 3rd order surface represents the basal bounding surface of this macroform. The horizontally stratified sand facies show 3rd order surface that truncates its own lower first order surfaces, which is well exhibited by huge troughs of >15 m. The cross-beds of this trough shows SSE palaeoflow. In the upper portion the change in lithofacies is observed marked by small trough of Gt-facies that are bounded by 2nd order surfaces.

This Sh_1-lithofacies marks the overbank deposition. The huge trough showing scouring of the horizontally stratified sand beds suggests channel avulsion in the overbank areas that flowed due SSE. The occurrence of the Gt-facies in the upper portion suggests change in flow regime from low to high energy.

SEDIMENTATION MODEL

The presence of such diverse lithofacies and their associations provide an insight to the nature of the older depositional systems, that persisted during the late Quaternary. Four principal phases of aggradation and stabilization are recognized. These phases relate to typical depositional style which mark their individuality.

Aggradation phase 1 : This aggradation phase marks the first fluvial sedimentation in the Mahi valley. It comprises the lithofacies viz. Gp, Sh, St and Gt of Rayka formation, that rests over the basal vertisol lithounit. The lithofacies suggests that the aggradation took place under low-sinuous braided channel complex (Miall, 1978) (Fig. 6.9 a, b, c), and in various depositional setting that gave rise to the development of different lithounits. These were resulted mainly due to downstream migration of straight crested transverse bars (Gp-facies), overbank sedimentation (Sh-facies), channel avulsion (St-facies), downstream migration of sinuous crested dunes, longitudinal bars alongwith minor channel fills (Gt-facies) (Fig. 6.9 b and c). The

Fig. 6.9a.

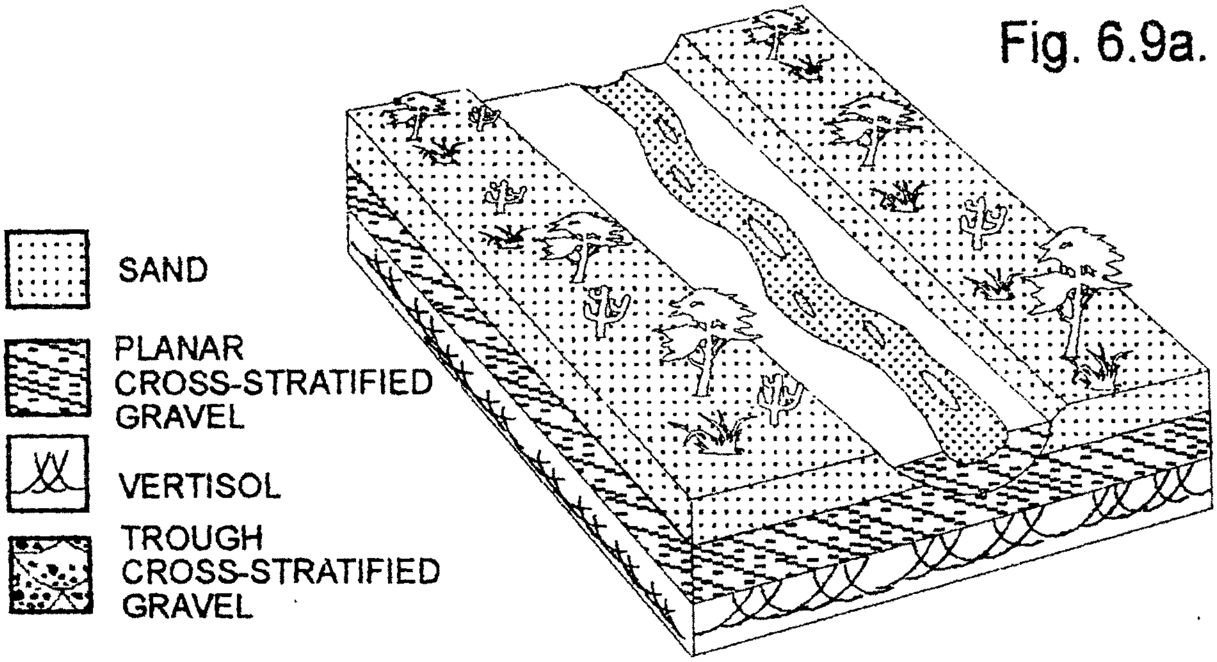

Moderate to low-sinuous river system. Marks the first fluvial sedimentation by shallow channels in Mahi valley at around 200 Ka B.P.

Fig.6.9b

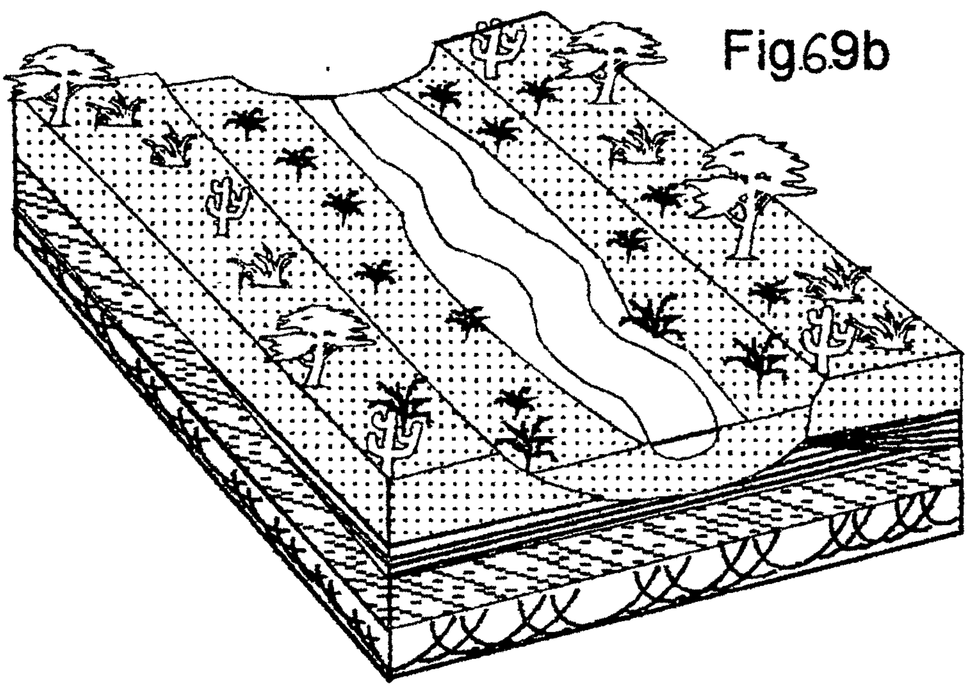

Overbank deposition in a broad and shallow channel with moderate sinuousity, calcrete layer formation in the floodplain area (?) around 120 ka B.P.

Fig. 6.9c

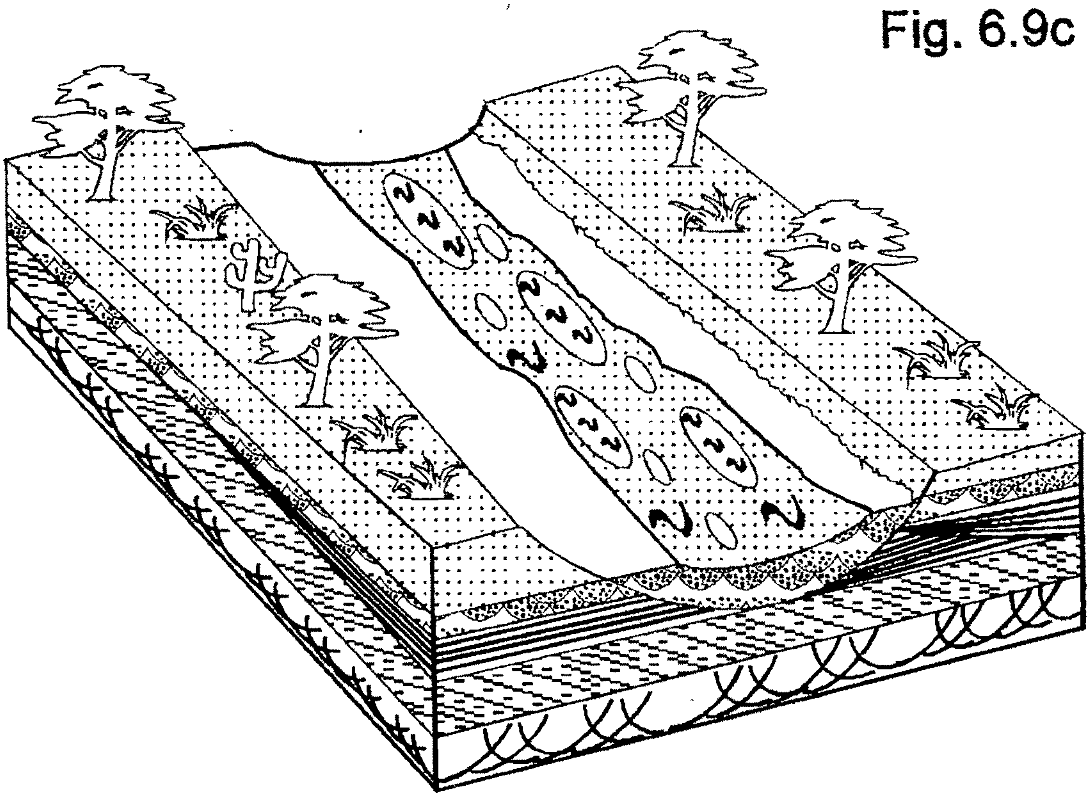

Braided river system at around ~108 ka when fluvial activity extended far downstream of present day mouth. Broad valley - shallow channel

Fig. 6.9d

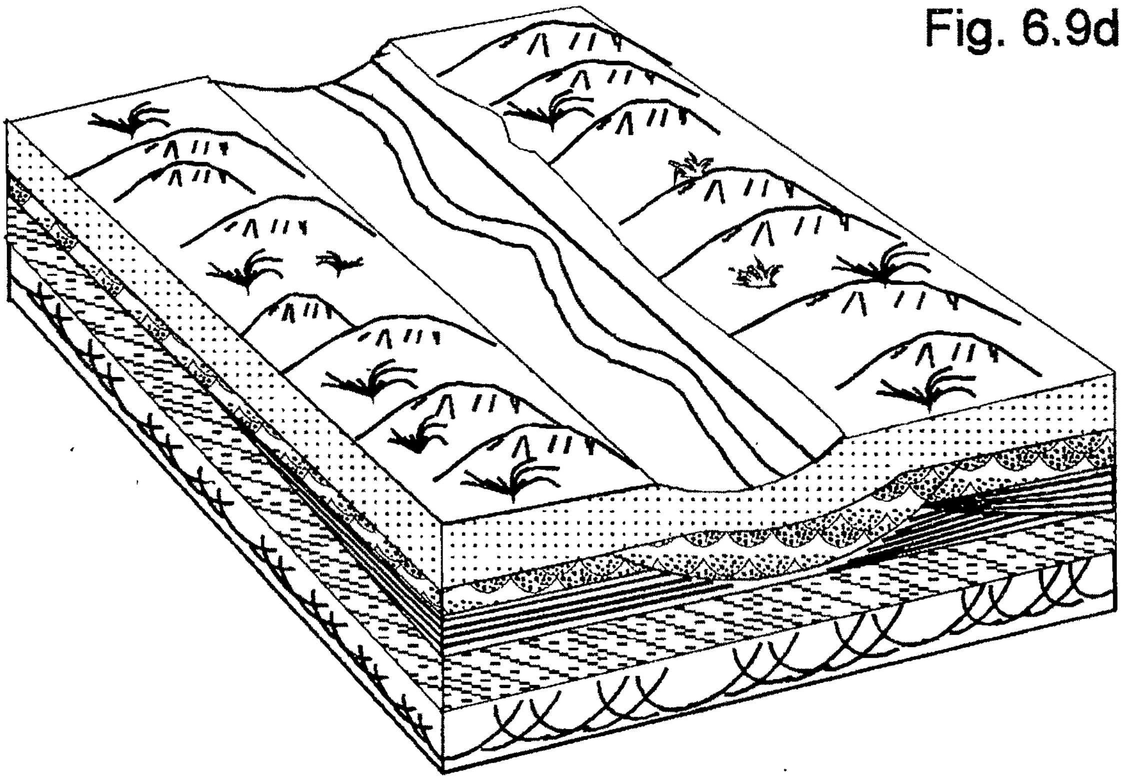

Shallow channel and narrow valley. Mainly sheetflood deposition between ~86 to 51 ka. Onset of aeolian activity around 18 ka channels were relatively shallow and were characterized by its high ephemeral nature, which is well manifested in the flow stage dependent magnitude of trough cross-stratas of Gt-facies. The concentration of calcrete clasts in the Gp and Gt lithofacies (in the lower reaches) as well as the petrographic studies suggest short distance transport from the near by source area in the upstream. The calcrete bed load must have been derived by the erosion of upstream banks probably within the alluvial plain. Such bank erosion took place during flashy discharges, which are commonly recorded in arid and semi-arid zone rivers (Miall, 1986). The change in the fluvial regime is well evidenced by the overlying Gt-facies, suggesting sudden increase in flow velocity and sediment influx in the area. Not much evidences of structures indicative of lateral accretion (LA), points toward the stability of the channels. The presence of vertisols on overbank facies suggests that bank cohesion was reasonably high. River waters were charged with carbonate in solution, which on drying created calcrete layers occurring parallel to the channel scours and are similar to palaeodrainage calcretes described by Arakel (1986).

Aggradation phase 2 : This aggradation phase marks the change in fluvial regime, where the flow velocity was reduced. This phase comprises mainly the multiple soil units overlying the sediment succession of aggradation phase 1 and represents the Shihora formation. During this phase the river mainly transported medium grained sands and silt, in a shallower channels. The occurrence of the trough cross-stratified conglomeratic lenses suggests presence of small scale channels. The river channels were shallow with a high width to height ratio (Fig. 6.9c). Difficulty of identifying channel banks at the exposures coupled with the facies character points to sheet-flooding to be a possible mechanism of aggradation (Friend, 1983). A high degree of ephemerality of the channel is well evidenced by the presence of horizontally stratified sand alongwith calcrete layers and multiple soil horizons. These lithounits suggests that the sedimentation was followed by a period of non-deposition/drier phase resulted into the pedogenesis and formation of calcrete layers. Formation of red-soil on both intra-channel and probable extra-channel deposits is indicative of infrequent sedimentation with intervening prolonged periods of pedogenesis.

Aggradation phase 3 *:* This phase marks the aeolian aggradation. The homogenous massive silts (Sim) dominate this period of sedimentation. It represents the Singrot formation. During this phase the channels were very shallow and valley width was narrowed down (Fig. 6.9d). The landscape was covered with aeolian dunes; water-laid deposits are not recognized in any of the sections studied. The aeolian sediments show characters similar to the classical loess sequences of Kashmir but have a lower silt percentage (Pant, 1993). Previous workers have preferred to call these sediments as 'loess-like'. Within this aeolian silt horizon periods of aggradation reflect dryness while intervening relatively humid periods are manifested as carbonate nodules. The absence of soil illuvial horizons might relate to shorter duration's of such stabilization events which curtailed horizonation.

Aggradation phase 4 *:* This phase represent the aggradation under new drainage network, that developed after the aeolian aggradation. This phase is marked by yet another fluvial sedimentation event and change in the climate from dry to humid. The new channel incised the older fluvial and aeolian sediment succession, and this was the period when the gully erosion started. The channel was comparatively narrow and had moderate to high sinuosity. During this aggradation contemporaneous fluvial (in the alluvial plain) and tidal/estuarine (in the coastal zone) sedimentation took place within the confined valley margins (Fig. 6.9e). The exposed fluvial and estuarine sediments comprises viz. Gp, Gt, Fl, Sp and Fsc lithofacies of the Kothiyakhad formation. The fluvio-marine sediments are suggestive of transgression of sea characterized by the inland migration of tidal inlet in a wide funnel shaped estuary. This followed degradation due to change in the base level and resulted into the incision of these deposits leading to the formation of unpaired terraces (Fig. 6.9 f).

Palaeocurrent directions were measured at some exposures and the results are illustrated in figure 6.10. At each site there is a discordance between measured directions and the present day flow path of the Mahi river. The data show the major flow trends SW, W and in the lower reaches it show SSE. The present day Mahi river is thus not responsible for the aggradation phases 1 and 2. Subsequent to these aggradation phases the area underwent structural adjustments. These are seen as sporadic occurrence of joints and small scale reverse faults in the sediment succession. A solitary instance of slickensides developed on a cliff face at Kadana indicates strike slip movement. Rosettes of lineament directions and present day channel-segment direction are similar proving that the present day younger Mahi channel follows the trends of these lineaments (Fig. 4.4 and Fig. 4.11). These lineaments formed through

Fig. 6.9e

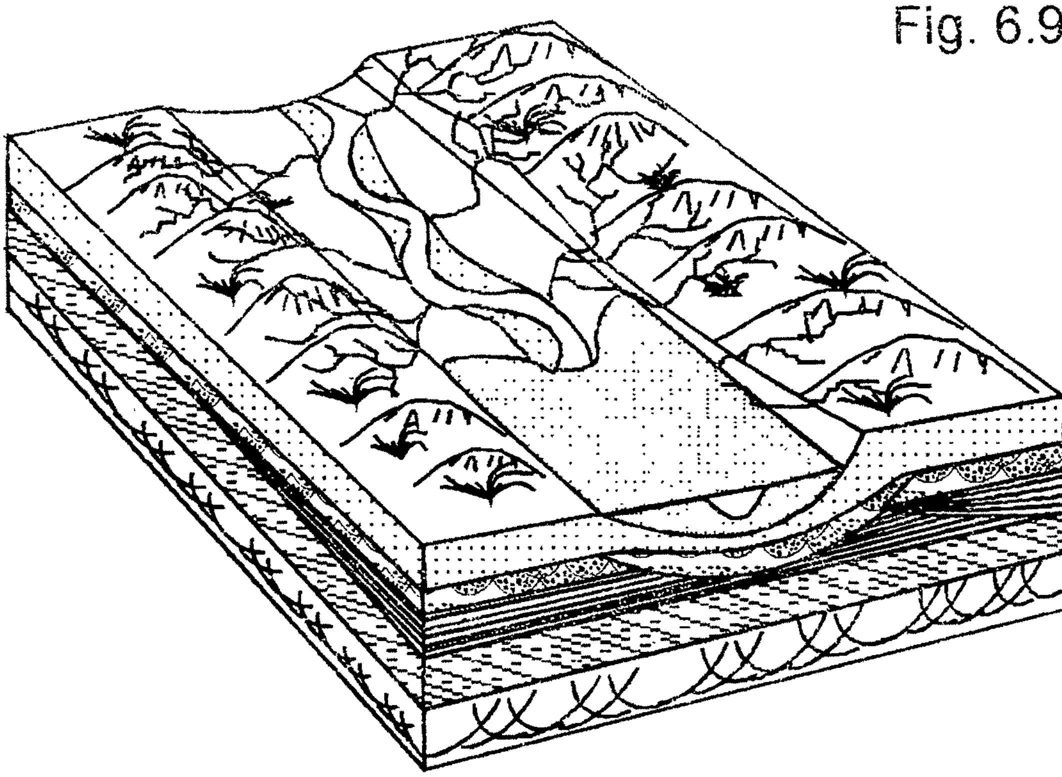

High sea level around 4 ka resulted in broadening of valley and landward migration of tidal inlet. Deposition of fluvial and tidal sediments.

Fig. 6.9f

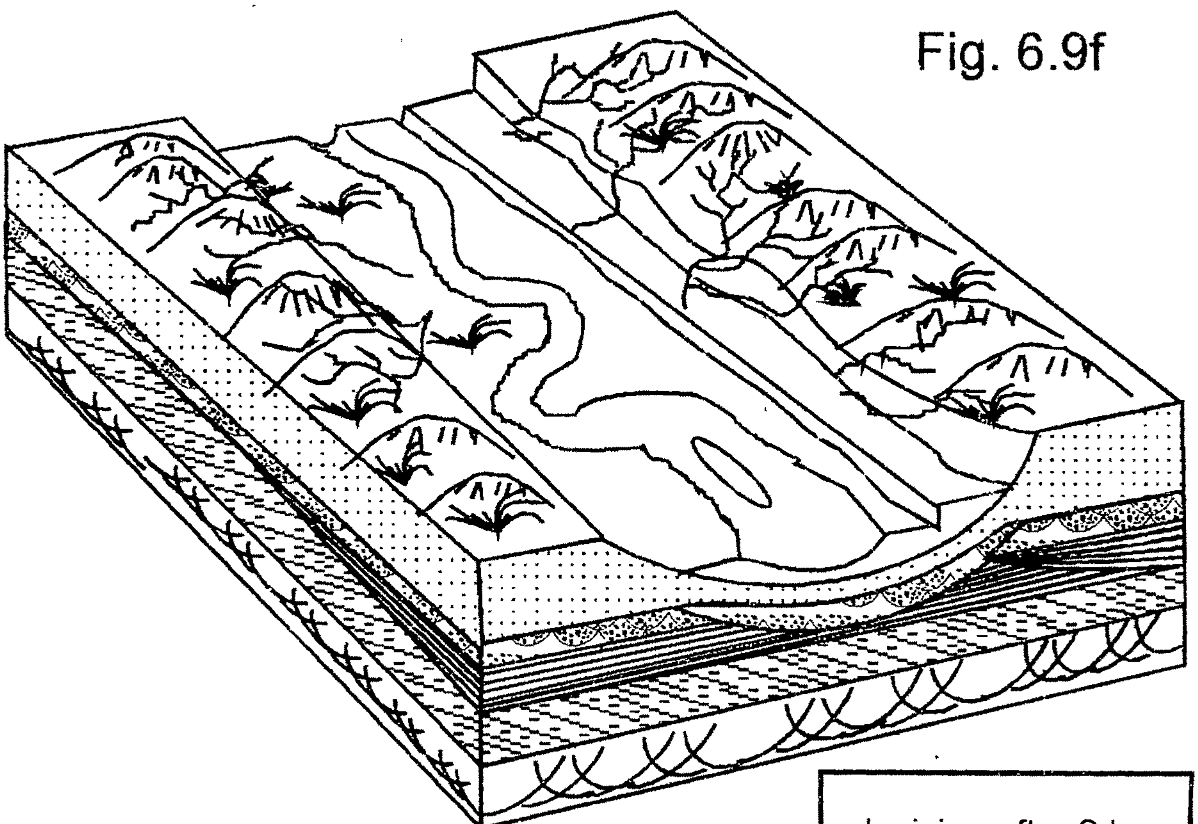

Incision after 2 ka

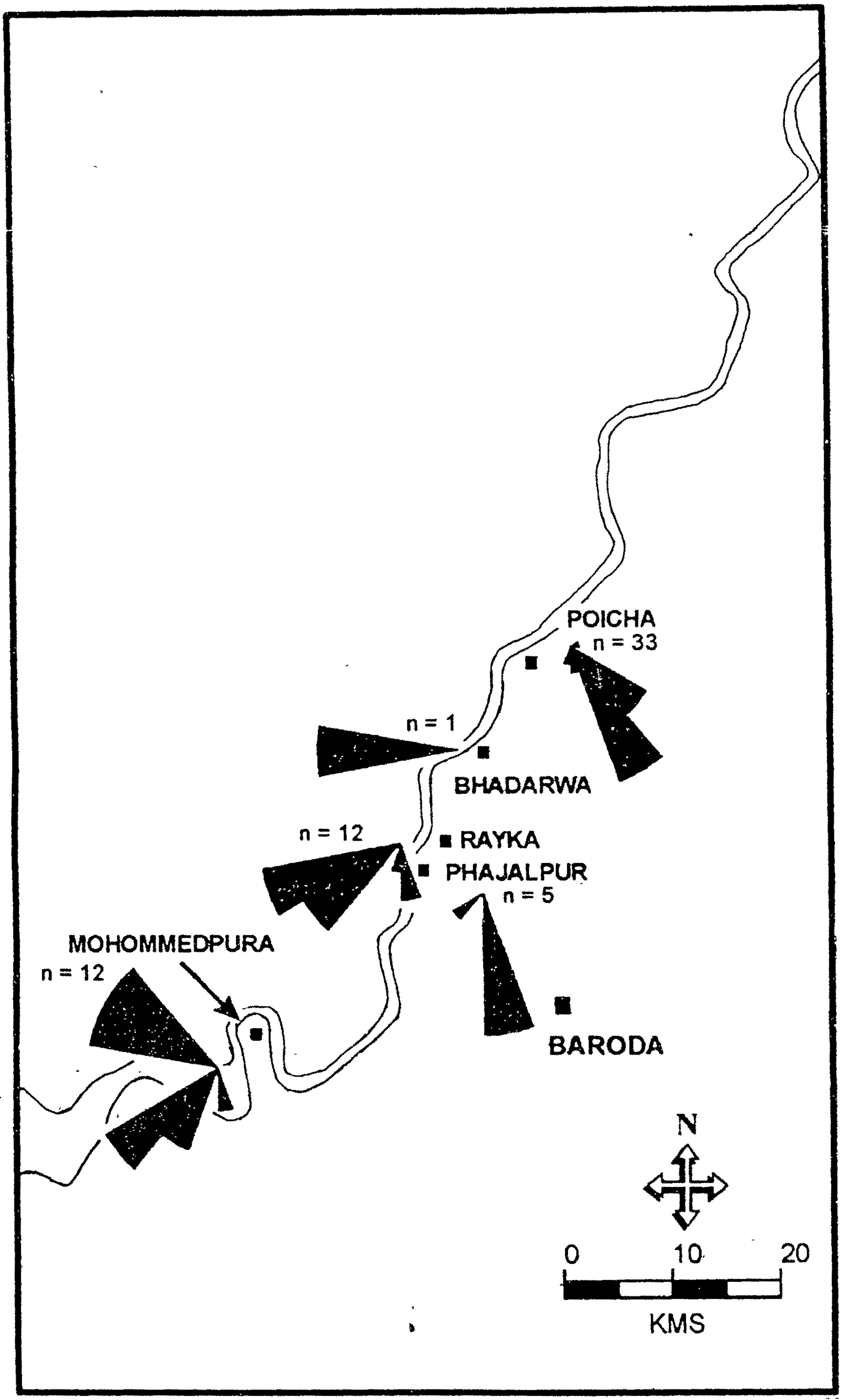

Fig. 6.10 : Palaeocurrent readings taken at various places

the re-activation of pre-Quaternary structures during the Mid-Holocene, after the aeolian aggradation 3. This re-activation could be related to the culmination of stresses accumulated through the northward movement of Indian plate (Khattri, 1994).